MARTIN MARIETTA ENERGY SYSTEMS LIBRARIES
3 4456 0361226 8

[redacted]

CENTRAL RESEARCH LIBRARY
DOCUMENT COLLECTION

ORNL-2441
C-84 - Reactors - Special Features of Aircraft Reactors cy 78A
M-3679 (20th ed., Rev.)

AEC RESEARCH AND DEVELOPMENT REPORT

DECLASSIFIED
CLASSIFICATION CHANGED TO:
BY AUTHORITY OF: AEC 5-7-70
BY: G. Goldberg 12-8-70

ORNL TUBE-FIN RADIATOR STRESS ANALYSIS

D. H. Platus

CENTRAL RESEARCH LIBRARY
DOCUMENT COLLECTION
LIBRARY LOAN COPY
DO NOT TRANSFER TO ANOTHER PERSON
If you wish someone else to see this document, send in name with document and the library will arrange a loan.

OAK RIDGE NATIONAL LABORATORY
operated by
UNION CARBIDE CORPORATION
for the
U.S. ATOMIC ENERGY COMMISSION

[redacted]

[redacted]

[redacted]

ORNL-2441
C-84 - Reactors - Special Features
of Aircraft Reactors
M-3679 (20th ed., Rev.)

This document consists of 66 pages.
Copy 78 of 227 copies. Series A.

Contract No. W-7405-eng-26

REACTOR PROJECTS DIVISION

ORNL TUBE-FIN RADIATOR STRESS ANALYSIS

D. H. Platus

DATE ISSUED

APR 1 - 1958

[redacted]

OAK RIDGE NATIONAL LABORATORY
Oak Ridge, Tennessee
operated by
UNION CARBIDE CORPORATION
for the
U.S. ATOMIC ENERGY COMMISSION

[redacted]

MARTIN MARIETTA ENERGY SYSTEMS LIBRARIES
3 4456 0361226 8

[redacted]

ORNL TUBE-FIN RADIATOR STRESS ANALYSIS

D. H. Platus

This report summarizes the stress analysis of the ORNL tube-fin radiator matrix. Specific problems considered include mechanical bending stresses resulting from air pressure and gravity loads and thermally induced stresses resulting from design and off-design temperature differentials within the tube-fin matrix. In certain critical areas where thermal stresses exceeded the elastic range of the structural material, a plastic strain analysis was undertaken in order to predict the structural life under strain-cycling conditions.

Air Pressure and Gravity Loads

Consider a section of the matrix free from forces so that the tubes are straight and parallel and tied together by fins running at right angles to the tubes (Fig. 1). Under uniformly applied loads the tubes will bend so as to remain parallel to each other as shown in Fig. 2. Since the fins are brazed to the tubes they will wrinkle as shown such that right angles are maintained at the tube-fin joints. The section of fin between adjacent tubes behaves as a beam fixed at both ends subjected to the forces and moments shown in Fig. 3. The slope of the fin, θ, at the fixed ends is equal to the slope of the tube. The resulting force transmitted to the tube consists only of a moment $2M_f$ since the forces, P, are equal and opposite (Fig. 4). An expression will be obtained for the value of the moment $2M_f$ which resists bending of the tubes and is directly proportional to the slope, θ, of the tube.

The deflection equation is

$$\frac{d^2y}{dx^2} = \frac{1}{D_f}(Px - M) \qquad (1)$$

where D_f is the flexual rigidity of the segment of fin. Integrating Eq (1)

[redacted]

and applying the boundary conditions $y'(o) = y'(s) = \theta$ and $y(o) = y(s) = 0$ gives an expression for M_f in terms of θ:

$$M_f = \frac{6D_f\theta}{s}$$

The total moment, M, resisting bending of the tubes is $2M_f$ so that

$$M = 2M_f = \frac{12D_f\theta}{s}$$

For n fins per unit length of tube, the resisting moment, M_x, per unit length is equal to $k\theta$ where

$$k = \frac{12nD_f}{s} \tag{2}$$

The problem is analogous to the classical "beam on elastic foundation" problem where in this case the resisting moment is proportional to the rotation of the beam.

A solution will be obtained for the general case of a cantilever beam with a uniformly distributed load and a concentrated moment and load applied to the free end (Fig. 5). The uniform load represents either air pressure or weight, and the end force and moment can be coupled with the slope and deflection of the free end for various end-support conditions. The moment at a distance x from the free end is given by

$$M(x) = M_o - Px - \frac{wx^2}{2} + \int_o^x M_x dx$$

where

$$\int_o^x M_x dx = k\int_o^x y'(x)dx = k\left[y(x) - y(o)\right]$$

so that

$$M(x) = M_o - Px - \frac{wx^2}{2} + k\left[y(x) - y(o)\right] \tag{3}$$

The deflection equation is

$$\frac{d^2y}{dx^2} = \frac{1}{D}\left[M_o - Px - \frac{wx^2}{2} + ky - ky_o\right]$$

Making the substitution $a^2 = k/D$,

$$\frac{dy^2}{dx^2} - ay = \frac{M_o}{D} - \frac{Px}{D} - \frac{wx^2}{2D} + a^2y_o \tag{4}$$

the general solution is seen to be

$$y = A \sinh ax + B \cosh ax + \frac{wx^2}{2k} + \frac{w}{a^2k} + y_o - \frac{M_o}{k} + \frac{Px}{k} \tag{5}$$

The following boundary conditions must be satisfied:

(i)	$y'(L) = 0$	(iii)	$y'(o) = \theta_o$
(ii)	$y(L) = 0$	(iv)	$y(o) = y_o$

Differentiating Eq (5), and applying the boundary conditions, the following expressions are obtained for the slope and deflection at the free end in terms of the applied loads:

$$k\theta_o \cosh aL + P(1 - \cosh aL) + \frac{w}{a}(aL - \sinh aL) + aM_o \sinh aL = 0 \tag{6}$$

$$k\theta_o \sinh aL + P(aL - \sinh aL) + \frac{w}{a}\left(1 - \cosh aL + \frac{a^2L^2}{2}\right) + aM_o(\cosh aL - 1) + y_o ak = 0 \tag{7}$$

Consider the ease of a free end where $P = 0$ and $M_o = 0$. From Eqs (6) and (7) the slope and deflection at the free end are given by

$$\theta_o = \frac{w}{ak}\left[\frac{\sinh aL - aL}{\cosh aL}\right] \tag{8}$$

$$y_o = \frac{w}{a^2k}\left[\frac{1 - \cosh aL}{\cosh aL} - \frac{a^2L^2}{2} + aL \tanh aL\right] \tag{9}$$

Combining these results with Eqs (3) and (5) the maximum bending moment at the fixed end is given by

$$M(L) = \frac{w}{a^2}\left[\frac{\cosh aL - 1}{\cosh aL} - aL \tanh aL\right] \tag{10}$$

Consider next the end condition where two tubes are tied together by a U-bend of tubing as shown in Fig. 6. By analogy with the deflection of the fin segment between adjacent tubes (Fig. 3), the section of U-bend will deform as shown in Fig. 7, and produce a resisting moment, M_o, which is proportional to the slope of the "free end" such that

$$M_o = k_o\theta_o \tag{11}$$

If the curvature in the bend is neglected, the constant, k_o, will be equal to $\frac{6D}{\lambda}0$, as calculated for the fins; λ is the distance between the tubes and D_o is the flexural rigidity of the connecting piece. Right angles are maintained as shown in Fig. 8.

The constant can be determined more accurately for two circular bends and a straight section subjected to a force and moment as shown in Fig. 9. From symmetry, $P = 2M_o/(\lambda + 2r)$ and there will be no rotation of the free end or deflection in the y-direction. The slope or rotation of the U-bend

is equal to $\delta_x/(\lambda + 2r)$ where δ_x is the deflection in the direction of the force P. By applying Castigliano's theorem of strain energy, δ_x is given by

$$\delta_x = \int_s \frac{M}{D} \frac{\partial M}{\partial P} ds \tag{12}$$

where the integral is taken over the total length, s, of the section. The integration yields for δ_x,

$$\delta_x = \frac{M_o}{\lambda + 2r} \left[\frac{1}{D_r} \left(\frac{\pi\lambda^2 r}{2} + \pi r^3 + 4\lambda r^2 \right) + \frac{\lambda^3}{6D_o} \right] \tag{13}$$

where D_o is the flexural rigidity of the straight section, λ_s, and D_r is the flexural rigidity of the curved sections corrected for the initial curvature. The correction is

$$D_r = \left(\frac{12h^2 + 1}{12h^2 + 10} \right) D_o$$

where

$$h = \frac{tr}{r_m^2}$$

and t is the tube wall thickness, r, the radius of bend and, r_m, the mean radius of tube.

The constant k_o is equal to $\frac{M_o}{(\lambda + 2r)\delta_x}$ or

$$k_o = \frac{(\quad + 2r)^2}{\frac{1}{D_r}\left(\frac{\pi\lambda^2 r}{2} + \pi r^3 + 4\lambda r^2\right) + \frac{\lambda^3}{6D_o}} \tag{14}$$

As r approaches zero this expression reduces to $6D_o/\lambda$ as calculated for the straight section only.

Applying this end condition (Eq 11) to Eqs (6) and (7), and solving for θ_o and y_o,

$$\theta_o = \frac{w}{ak}\left[\frac{\sinh aL - aL}{\cosh aL + \frac{ak_o}{k}\sinh aL}\right] \tag{15}$$

$$y_o = \frac{w}{a^2k}\left[\frac{\frac{a^2Lk_o}{k}(\cosh aL - 1) + aL\sinh aL - \cosh aL + 1}{\cosh aL + \frac{ak_o}{k}\sinh aL} - \frac{a^2L^2}{2}\right] \tag{16}$$

Combining these results with Eqs (3) and (5), the maximum bending moment at the fixed end is given by

$$M(L) = \frac{w}{a^2}\left[1 - \frac{1 + aL\sinh aL + \frac{a^2Lk_o}{k}\cosh aL}{\cosh aL + \frac{ak_o}{k}\sinh aL}\right] \tag{17}$$

The maximum stress, $\frac{M(L)r_o}{I_o}$, is plotted in Fig. 10 as a function of the dimensionless parameter, aL, for dimensions indicated on the figure. The broken-line curve represents the U-bend condition, Eq (17), and the solid curve represents the free end condition, Eq (10). It is seen from the figure that, for the dimensions indicated, the U-bend offers no support for values of aL greater than 3.

For the case of a pinned end with the U-bend condition (Fig. 11), $y_o = 0$ and the slope at the pinned end, from Eq (7), is

$$\theta_o = \frac{P(\cosh aL - 1) + \frac{w}{a}(\sinh aL - aL)}{k\cosh aL + ak_o\sinh aL} \quad . \tag{18}$$

The maximum bending moment at the fixed end from Eqs (3) and (5) is

$$M(L) = P\left[\frac{k_o(1-\cosh aL) - \frac{k}{a}\sinh aL}{k\cosh aL + ak_o\sinh aL}\right] + \frac{w}{a}\left[\frac{\frac{k}{a}(\cosh aL - 1 - aL\sinh aL) + k_o(\sinh aL - aL\cosh aL)}{k\cosh aL + ak_o\sinh aL}\right] \quad (19)$$

The reaction, P, at the pinned end is obtained by substituting Eq (18) into Eq (7).

$$P = \frac{w}{a}\left[\frac{1-\cosh aL - \frac{a^2L^2}{2}\cosh aL + aL\sinh aL + \frac{a^2Lk_o}{k}(\cosh aL - 1 - \frac{aL}{2}\sinh aL)}{\frac{2ak_o}{k}(1 - \cosh aL + \frac{aL}{2}\sinh aL) + aL\cosh aL - \sinh aL}\right] \quad (20)$$

Consider next the case where the fins do not extend all the way to the headers so that there is a section, ℓ, of unfinned tube as shown in Fig. 12. The moment of inertia of the finned tube will be greater than that of the unfinned tube because of the fin collar thickness and brazing alloy. The flexural rigidities will be represented by D and D_o for the finned and unfinned tubes, respectively. A solution will be obtained for the case of a concentrated end load, P, with the U-bend boundary condition.

The deflection Eq (4) is solved for the finned span with the following boundary conditions:

(i) $y(o) \equiv y_o$ (iii) $y(L) \equiv 0$

(ii) $y'(o) \equiv \theta_o = \frac{M_o}{k_o}$ (iv) $y'(L) \equiv \theta_L$

The bending moment M(L) at the end of the finned section is obtained as a function of θ_L:

$$M_L = \frac{\alpha}{a}\left[k\theta_L + P(\cosh aL - 1) + w(\frac{1}{a}\sinh aL - L)\right] - \frac{P}{a}\sinh aL - \frac{w}{a^2}(\cosh aL - 1) \quad (21)$$

where

$$\alpha \equiv \frac{\frac{k}{ak_o} \sinh aL + \cosh aL}{\frac{k}{ak_o} \cosh aL + \sinh aL} \tag{22}$$

The deflection at x = 0 is

$$y_o = \frac{\theta_L + \frac{P}{k}(\cosh aL - 1) + \frac{w}{k}\left(\frac{1}{a}\sinh aL - L\right)}{\frac{k}{k_o} \cosh aL + a \sinh aL} - \frac{M_L}{k} - \frac{wL^2}{2k} - \frac{PL}{k} \tag{23}$$

For the unfinned span, Fig. 13, the slope and deflection at the free end are

$$\theta_L = \frac{1}{D_o}\left(\frac{P\ell^2}{2} + \frac{wL\ell^2}{2} - M_L\ell\right) \tag{24}$$

$$y_L = \frac{1}{D_o}\left(\frac{M_L\ell^2}{2} - \frac{P\ell^3}{3} - \frac{wL\ell^3}{3}\right) \tag{25}$$

and the maximum moment at the fixed end is

$$M_\ell = M_\ell - wL\ell - P\ell \tag{26}$$

Substituting Eq (24) into Eqs (21) and (23),

$$M_L = \left(\frac{1}{1+\frac{\alpha k\ell}{aD_o}}\right)\left\{\frac{P}{a}\left[\frac{\alpha k\ell^2}{2D_o} + \alpha(\cosh aL - 1) - \sinh aL\right] + \frac{w}{a^2}\left[\frac{\alpha ak\ell^2 L}{2D_o} + \alpha(\sinh aL - aL) - \cosh aL + 1\right]\right\} \tag{27}$$

and

$$y_o = \frac{P\left(\frac{\ell^2}{2D_o} + \frac{\cosh aL - 1}{k}\right) + w\left(\frac{\ell^2 L}{2D_o} + \frac{\sinh aL - aL}{a\,k}\right) - \frac{M_L}{D_o}}{\frac{k}{k_o}\cosh aL + a \sinh aL} - \frac{1}{k}\left(M_L + PL + \frac{wL^2}{2}\right) \tag{28}$$

The total deflection of the free end is $y_o + y_L$.

Numerical Solution

A numerical solution is carried out for the case shown in Fig. 12, but for four U-bends tied together as shown in Fig. 14. Assuming that the four tubes remain parallel during bending, the spring constant (Eq. 2) will be reduced by 1/4 since only three segments of fin undergo bending for the four tubes. Therefore

$$k = \frac{9nD_f}{s} \tag{29}$$

The tube dimensions are:

r_m = 0.08125 $\qquad I_o = 0.4312\text{x}10^{-4}$ in^4

r_i = 0.06875 in. $\qquad I = 0.7345\text{x}10^{-4}$ in^4

r_o = 0.09375 in. (unfinned tube)

r_f = 0.10375 in. (finned tube)

Fin Dimensions:

The tubes are arranged in a square array with 2/3 in. between centers (Fig. 16). The section of fin (per tube) which undergoes bending is shown by the dotted lines. The width of the section, b, is 2/3 in. and the length, s, has been approximated by $(2/3 - r_f)$ or 0.5629 in. The fins are a sandwich of stainless-steel clad copper (0.0025 - 0.005 - 0.0025 in.). Assuming the copper has no structural value, the moment of inertia of the section is (from Fig. 17):

$$I_f = \frac{2b}{3}(y_2^3 - y_1^3)$$

For $y_2 = 0.005$ in.
$y_1 = 0.0025$ in.
$I_f = 4.105\text{x}10^{-8}$ in^4

From Eq (29) with n = 15 fins/in.,

$$k = \frac{9nI_fE}{s} = 9.845\text{x}10^{-6}E$$

U-bend Spring Constant:

From Fig. 9 the radii of the two bends are 5/8 in. and the straight section, λ , is 2.625 in. The curvature correction constant is

$$h = \frac{tr}{r_m^2} = \frac{(0.025)(0.625)}{(0.08125)^2} = 2.367$$

and

$$D_r = \left(\frac{12h^2 + 1}{12h^2 + 10}\right) D_o = 0.8835\ EI_o = 0.3810\text{x}10^{-4}E$$

The constant k_o is (from Eq 14)

$$k_o = \frac{(\lambda + 2r)^2}{\frac{1}{D_r}\left(\frac{\pi\lambda^2 r}{2} + \pi r^3 + 4\lambda r^2 + \frac{\lambda^3}{6D_o}\right.} = 40.04\text{x}10^{-6}E$$

The constant, a, which relates the fin stiffness to that of the tube, is

$$a = \sqrt{\frac{k}{D}} = \sqrt{\frac{9.845\text{x}10^{-6}E}{0.7345\text{x}10^{-4}E}} = 0.3661\ \text{in}^{-1}$$

The bending stresses and deflections for the case shown in Fig. 12 will be computed for L = 15 in. and ℓ = 1.25 in.

$$aL = 5.492 \qquad \sinh aL = \cosh aL = 121$$

From Eq (22), $\alpha = 1$, and Eq (27) reduces to

$$M_L = \left(\frac{1}{1 + \frac{k\ell}{aD_o}}\right)\left[\frac{P}{a}\left(\frac{k^2}{2D_o} - 1\right) + \frac{w}{a^2}\left(\frac{ak^2L}{2D_o} - aL + 1\right)\right] \quad (30)$$

Substituting the numerical values,

$$M_L = \left(\frac{1}{1.780}\right)\left[-2.244\ P - 26.19\ w\right]$$

$$= -1.260\ P - 14.71\ w \text{ lb-in.}$$

From Eq (26), the bending moment at the tube-header joint is

$$M_\ell = M_L - w\ell L - P\ell$$

$$= -2.51\ P - 33.46\ w \text{ lb-in.}$$

The moments are in units of lb-in. for the concentrated load P in lb. and a distributed load w in lb/in. The corresponding maximum bending stresses are given by

$$\sigma_{max} = \frac{Mr_{max}}{I} \quad .$$

For the finned tubing $r_{max}/I = 1412$ and for the unfinned tubing $r_{max}/I_o = 2174$. The maximum stress in the finned tubing is:

$$\sigma_L^{(f)} = 1412\ M_L = -1779\ P - 20{,}770\ w$$

The stress in the unfinned tubing adjacent to the fins is:

$$\sigma_L^{(0)} = 2174\ M_L = -\ 2739\ P - 31{,}980\ w$$

The maximum stress in the unfinned tubing at the tube-header joint is:

$$\sigma_\ell^{(0)} = 2174\ M_\ell = -\ 5457\ P - 72{,}740\ w$$

The distributed load, w, for the weight of the matrix is estimated as follows:

Material	Volume/ in. of tube	Density	Weight/in.
Inconel	0.01276 in^3	526 lb/ft^3	0.00389 lb/in
Stainless Steel	0.03238 "	492 "	0.00922 "
Copper	0.03238 "	556 "	0.01042 "
NaK	0.01485 "	46 "	0.00040 "
Braze Alloy (assume 0.010 in.)	0.00620 "	526 "	0.00189 "
		Total	0.0258 lb/in

With no end support, P = 0, and the corresponding stresses from the weight of the matrix are (refer to Fig. 18)

$$\sigma_L^{(f)} = 536 \text{ psi} \qquad \sigma_L^{(0)} = 825 \text{ psi} \qquad \sigma_\ell^{(0)} = 1877 \text{ psi}$$

It should be noted that the maximum stress at the tube header joint is a factor of 3.5 greater than the maximum stress in the brazing alloy where the fins begin and a factor of 2.3 greater than the stress in the unfinned tube adjacent to the fins.

The air drag load behaves as a uniformly distributed load similar to the weight load. Its magnitude is estimated as follows:

Flow area = 30x15 = 450 in^2

Total number of tubes = 45x8 = 360

Length of tube = 15 in.

For h in. of H_2O air pressure drop,

$$w = \frac{(h\ in)(62.4\ lb/ft^3)(450\ in^2)}{(360\ tubes)(15\ in/tube)(1728\ in^3/ft^3)} = 3.009x10^{-3}\ h(lb/in)$$

For a design pressure drop of 8 in H_2O, w = 0.0241 lb/in.

The corresponding bending stresses are

$$\sigma_L^{(f)} = 501\ psi \qquad \sigma_L^{(o)} = 771\ psi \qquad \sigma_\ell^{(o)} = 1753\ psi$$

For bending in a direction parallel to the headers the tubes are tied together by the fins in 5-tube groups (Fig. 19). The fin spring constant (Eq 2) will be reduced by a factor of 4/5 so that

$$k = \frac{48}{5}\left(\frac{nD_f}{s}\right) = 10.50x10^{-6}E$$

The U-bends provide no support for deflection in the direction shown so that $k_o = 0$, and from Eq (22) $\alpha = \tanh aL$.

$$a = \sqrt{\frac{k}{D}} = \sqrt{\frac{10.50x10^{-6}}{0.7345x10^{-4}}} = 0.3781$$

$$aL = 5.672 \qquad \text{and} \qquad \tanh aL \simeq 1.$$

Equation (27) reduces to Eq (30). Substituting the numerical values,

$$M_L = \left(\frac{1}{1.805}\right)\left[-2.142\ P - 25.13\ w\right] = -1.187\ P - 13.92\ w$$

$$M_\ell = -2.437\ P - 32.67\ w \quad .$$

The corresponding stresses for the distributed weight load, w = 0.0258 lb/in., are

$$\sigma_L^{(f)} = 507 \text{ psi} \qquad \sigma_L^{(0)} = 781 \text{ psi} \qquad \sigma_\ell^{(0)} = 1832 \text{ psi}$$

The combined air and weight loads will produce a resultant load determined by the vector sum of the two loads. Since bending will not take place along one of the two principal directions of the square matrix the spring constant of the fins cannot be readily determined as in Fig. 16. Also, bending in one of the principal directions would produce a wrinkling of the fins which would resist bending in the other principal direction. As a first approximation the maximum stress will be taken as the vector sum of the two bending stresses although both effects mentioned above will tend to make this a conservative estimate.

$$\sigma_{L\ max}^{(f)} = \sqrt{(507)^2 + (501)^2} = 713 \text{ psi}$$

$$\sigma_{L\ max}^{(0)} = \sqrt{(781)^2 + (771)^2} = 1097 \text{ psi}$$

$$\sigma_{\ell\ max}^{(0)} = \sqrt{(1832)^2 + (1753)^2} = 2536 \text{ psi} \quad .$$

A curve showing the creep properties of Inconel at 1500°F is included in Fig. 20 for an estimate of the creep life under the maximum predicted bending stress. This data was obtained from a tensile creep test and does not strictly apply to the condition of creep in bending. It has been shown that during creep bending the forces redistribute themselves over the beam cross section in such a manner as to relieve the outermost fiber stresses and thus increase the creep life[1]. The equivalent tensile stress may be 70 to 80 percent of the maximum bending stress, predicted from elastic theory, for comparable strain rates, depending on the geometry and material properties.

---

1. D. L. Platus, Stress Analysis of a Heat Exchanger Tube in Creep Bending, ORNL CF 57-2-101 (February 22, 1957).

[redacted]

Thermally Induced Stresses

Consider first the stresses resulting from temperature differences between adjacent tubes in the matrix. As the air gains heat in passing through the radiator the driving potential for heat transfer is reduced and there will be a temperature increase between successive tubes in the direction of air flow. If there were no restraints from fin interactions the tubes would deform as shown in Fig. 19 where $\overline{T}$ represents an average temperature over the span L and α is the coefficient of thermal expansion of the tube. As a result of fin interactions, discussed in the previous section, the tubes will deform as shown in Fig. 22. If we assume that the temperature difference between adjacent tubes is constant at any point, x, along the span of the tube, then all tubes will bend so as to remain parallel to each other. We can then isolate one tube from the matrix and examine the bending stresses induced in the tube from the temperature differentials.

Consider two adjacent tubes differing in temperature by an amount $\Delta T(x)$. If the tubes did not bend the fins would be deflected as shown in Fig. 22 and exert a moment on the tube equal to $k\theta_t(x)$, where k is defined in Eq (2), and

$$\theta_t(x) = \frac{\alpha}{s} \int_x^L T(x')dx' \qquad (31)$$

Tue tubes will bend to partially relieve the stress in the fins so that the actual slope at any point x is $\theta(x)$ and the distributed moment, M_x, acting on the tubes is proportional to the slope of the fin section and is given by

$$M_x = k\left[\theta(x) - \theta_t(x)\right]. \qquad (32)$$

The problem is identical to that previously considered with the addition of the term $\theta_t(x)$.

[redacted]

The total moment acting on the tube from the fin reaction is

$$\int_o^x M_x dx' = k\left[y(x) - y(o) - \int_o^x \theta_t(x')dx'\right]$$

If we let $\Delta T(x) = \Delta T$ = constant, then

$$\theta_t(x) = \frac{\alpha\Delta T}{s}(L - x)$$

and

$$\int_o^x \theta_t(x')dx' = \frac{\alpha\Delta T}{s}\left(Lx - \frac{x^2}{2}\right)$$

Neglecting the distributed load, w, and concentrated load, P, in Fig. 5, the deflection equation becomes

$$\frac{dy^2}{dx^2} - ay^2 = \frac{M_o}{D} - a^2\left[y_o + \frac{\alpha\Delta T}{s}\left(Lx - \frac{x^2}{2}\right)\right] \qquad (33)$$

From the radiator configuration shown in Fig. 14, the matrix consists of two banks of tubes connected by U-bends. The average tube temperature in one bank will differ from the average tube temperature in the other by an amount ΔT_b and, by analogy with the fin deflection in Fig. 22, the moment exerted on the end of the tube from the U-bend will be given by

$$M_o = k_o\left[\theta(o) - \theta t(o)\right]$$

where k_o is given in Eq (14) and, from Fig. 9,

$$\theta_t(o) = \frac{\alpha\Delta T_L L}{\lambda + 2r} \quad .$$

Applying this boundary condition plus the condition of zero slope and deflection at the fixed end, the solution of Eq (33) yields for the maximum bending moment at the fixed end,

$$M(L) = \frac{-k_o\theta_t(o) + \frac{\alpha\Delta T}{a\,s}\left[\frac{k}{a}(1 - \cosh aL) + k_o(aL - \sinh aL)\right]}{\cosh aL + \frac{ak_o}{k}\sinh aL} \qquad (34)$$

Numerical Solution

Substituting the numerical results from the previous calculation into Eq (34) gives the maximum bending stress in the unfinned tube in terms of ΔT and ΔT_b. For the following dimensions and constants:

$a = 0.3661\ in^{-1}$	$\alpha = 10^{-5}\ in/in^{o}F$	$I_o = 0.4312x10^{-4} in^4$
$L = 15$ in.	$s = 0.5629$ in.	$r_o = 0.09375$ in.
$k = 9.845x10^{-6}E$	$\lambda + 2r = 3.875$ in.	$k_o = 40.04x10^{-6}E$
		$E = 20x10^6$ psi

$$\sigma_L^{(0)} = \frac{M(L)r_o}{I_o} = 55.02\,\Delta T + 0.2238\,\Delta T_b \quad .$$

Figure 23 gives some estimated tube temperatures at normal operating conditions[2]. Average values for ΔT and ΔT_b are on the order of 30^oF and 200^oF, respectively, which result in a value of 1700 psi for $\sigma_L^{(0)}$.

The next thermal stress problem to be evaluated is that resulting from a condition in which the temperature of one tube in the matrix differs from the average temperature of adjacent tubes. Such a condition might occur from mass transfer within the fluid system which would deposit solid material on the tube wall and restrict the coolant flow. As a result, the temperature of the plugged tube could be considerably lower than the temperature of adjacent tubes.

2. Calculated by R. I. Gray, December 14, 1955.

The problem will be analyzed by considering the fin sections surrounding the cold tube as circular diaphrams. As the tube contracts, each diaphram will exert a force on the tube, tending to pull it from the header. Figure 24 shows the deflection of one fin section at a distance x from the header as the tube is cooled an amount T degrees below the temperature of the surrounding tubes. The diaphram deflects by an amount $\delta(x)$ and the tube is displaced an amount u(x) from the cold, unrestrained position. From Fig. 24

$$\alpha \Delta T x = u(x) + \delta(x) \tag{35}$$

If we examine an incremental segment of tubing we will note that the tensile force in the tube, P(x), is increased by an amount F(x) per unit length in the direction of the header due to the action in the fins. From Fig. 25

$$F(x) = -\frac{dP}{dx} \quad . \tag{36}$$

Since the fin force is proportional to the deflection of the fins, $\delta(x)$,

$$F(x) = K\delta(x) = -\frac{dP}{dx} \tag{37}$$

where K is the spring constant per unit length of tube and is equal to the product of the number of fins per unit length, n, and the spring constant of the individual fin diaphram, k.

From Hook's law,

$$P(x) = AE\epsilon(x) = AE\frac{du}{dx} \tag{38}$$

where A and E are the tube cross sectional area and modulus of elasticity, respectively, and $\epsilon(x)$ is the strain at the position x. Differentiating Eqs (38) and substituting into Eq (37),

$$\delta(x) = -\frac{AE}{K}\frac{du^2}{dx^2} \tag{39}$$

Combining this expression with Eq (35) gives the deflection equation for the tube,

$$\frac{du^2}{dx^2} - \eta^2 u = - \alpha \Delta T \eta^2 x \tag{40}$$

where

$$\eta^2 = \frac{K}{EA} = \frac{nk}{EA} \tag{41}$$

The solution of Eq (40) is

$$u(x) = C_1 \sinh \eta x + C_2 \cosh \eta x + \alpha \Delta T x \tag{42}$$

The constants C_1 and C_2 are obtained from the end restraints on the tube. For the first case consider a length L of finned tubing fixed at the header and free at the opposite end. These conditions require that the displacement be zero at the fixed end and the tensile force be zero at the free end. From the first condition,

$$u(o) = 0 = C_2 \quad .$$

From the second condition,

$$P(L) = EA \left(\frac{du}{dx}\right)_{x=L} = 0 \quad .$$

Differentiating Eq (42) and applying this condition gives for C_1,

$$C_1 = - \frac{\alpha \Delta T}{\eta \cosh \eta L} \quad .$$

The solution for displacement as a function of x is then

$$u(x) = \alpha \Delta T \left(x - \frac{\sinh \eta x}{\eta \cosh \eta x}\right. \quad . \tag{43}$$

From Eq (38), the tensile stress as a function of x is

$$\sigma(x) = E \frac{du}{dx}$$

and by differentiating Eq (43),

$$\sigma(x) = \alpha E \Delta T \left(1 - \frac{\cosh \eta x}{\cosh \eta L}\right) \quad . \tag{44}$$

It is seen from this result that the stress increases from zero at the free end to a maximum value at the fixed end given by

$$\sigma(o) = \alpha E \Delta T \left(1 - \frac{1}{\cosh \eta L}\right) \tag{45}$$

The term in parenthesis is a fraction and will approach the value of unity as the stiffness of the fins becomes infinitely large. In the limit the maximum stress is $\alpha E \Delta T$ for a completely rigid matrix. The maximum stress is plotted in Fig. 26 as a function of ηL.

For a second case of end restraints we consider the configuration shown in Fig. 12 where a small segment ℓ of unfinned tubing connects the fin matrix to the header. If x is the distance measured from the beginning of the finned matrix outward from the header, then the second condition of the previous case still holds for the free end. The first condition must account for the deflection of the segment ℓ of tube from the action of the constant load P(o). If A_o is the cross-sectional area of this section of tube (which is less than the cross-sectional area, A, of the finned tube by an amount equal to the area of the fin collar plus brazing alloy) then the displacement at x = 0 is given by

$$u(o) = \frac{P(o)\ell}{A_o E} - \alpha \ell \Delta T_\ell \tag{46}$$

where ΔT_ℓ is the temperature differential of the unfinned tube. If we take $\Delta T_\ell = \Delta T$ = constant and solve for C_1 and C_2 from the free-end condition and Eq (46), Eq (42) gives for the displacement

$$u(x) = \frac{\alpha \Delta T}{\eta} \left[\frac{\frac{A_o}{A}(\eta \ell \sinh \eta L - 1) - \eta \ell \sinh \eta L}{\frac{A_o}{A} \cosh \eta L + \eta \ell \sinh \eta L} \right] \sinh \eta x + \alpha \Delta T \ell \left[\frac{(1 - \frac{A_o}{A}) \cosh \eta L - 1}{\frac{A_o}{A} \cosh \eta L + \eta \ell \sinh \eta L} \right] \cosh \eta x + \alpha \Delta T x \tag{47}$$

Differentiating this result, the stress in the finned portion of tube $\frac{P(x)}{A}$, is, from Eq (38),

$$\sigma(x) = \alpha E \Delta T \left[\frac{\left(\frac{A_o}{A} - 1\right)\eta \ell \sinh \eta L - \frac{A_o}{A}}{\frac{A_o}{A}\cosh \eta L + \eta \ell \sinh \eta L} \right] \cosh \eta x + \tag{48}$$

$$\alpha E \Delta T \eta \ell \left[\frac{1 - \frac{A_o}{A} \cosh L - 1}{\frac{A_o}{A} \cosh L + \sinh L} \right] \sinh \eta x + \alpha E \Delta T$$

The maximum stress occurs in the unfinned portion and is constant over the length ℓ. From Eq (48),

$$\sigma_{max} = \frac{A}{A_o} \sigma(o) = \alpha E \Delta T \left[\frac{\cosh \eta L + \eta \ell \sinh \eta L - 1}{\frac{A_o}{A} \cosh \eta L + \eta \ell \sinh \eta L} \right] \tag{49}$$

Because of the reduced area of the unfinned tube, the maximum stress can exceed the value of $\alpha E \Delta T$ which was seen to be the limiting stress in the previous case. In the limit as A/A_o approaches unity and ℓ approaches acro, Eq (49) reduces to Eq (45). If the temperature differential between the cold tube and surrounding tubes is given by some function of x along the tube then Eq (35) becomes

$$\alpha \int_o^x \Delta T(x')dx' = u(x) + \delta(x) \tag{50}$$

For the case of a linear gradient increasing from zero at the header to ΔT_L at $x = L$, $\Delta T(x)$ is given by

$$\Delta T(x) = \frac{\Delta T_L x}{L}$$

and the general solution for deflection corresponding to Eq (42) is

$$u(x) = C_1 \sinh \eta x + C_2 \cosh \eta x + \frac{\alpha \Delta T_L x^2}{2L} + \frac{\alpha \Delta T_L}{\eta^2 L} \tag{51}$$

For the previous conditions of zero displacement at the fixed end and zero tensile force at the free end, the deflection equation becomes

$$u(x) = \frac{\alpha\Delta T_L}{2_L}\left(\frac{\sinh \eta L - \eta L}{\cosh \eta L}\right) \sinh \eta x - \frac{\alpha\Delta T_L}{\eta 2_L} (\cosh \eta x - 1) + \frac{\alpha\Delta T_L x^2}{2L} \qquad (52)$$

and the maximum stress at the fixed end is

$$\sigma(o) = \alpha E\Delta T_L \left(\frac{\sinh \eta L - \eta L}{\eta L \cosh \eta L}\right) \qquad (53)$$

This result is plotted in Fig. 27 as a function of ηL.

For the case of the unfinned tube section with a linear temperature gradient, if $\Delta T_\ell = 0$ so that the temperature differential begins at the fin matrix, then the maximum stress in the unfinned tube from Eqs (46) and (51) is given by

$$\sigma_{max} = \frac{P(o)}{A_o} = \frac{\alpha E\Delta T_L A}{\eta L A_o} \left(\frac{\sinh \eta L - \eta L}{\cosh \eta L + \frac{\eta \ell A}{A_o} \sinh \eta L}\right) \qquad (54)$$

An expression will be obtained for the deflection u(o) as a function of the tensile force P(o) in the unfinned tube to be used in conjunction with a plastic strain analysis of the unfinned tube portion. If we define u(o) as u_o and use this boundary condition along with the free end condition, the tensile force P(o) for the case of constant ΔT is given by

$$P(o) = \alpha EA\Delta T \left(\frac{\cosh \eta L - 1}{\cosh \eta L}\right) - \eta EAu_o \tanh \eta L \qquad (55)$$

For the linear temperature differential,

$$P(o) = \frac{\alpha EA\Delta T_L}{\eta L} \left(\frac{\sinh \eta L - \eta L}{\cosh \eta L}\right) - \eta EAu_o \tanh \eta L \qquad (56)$$

The spring constant, k, of a circular diaphram fixed at the inner and outer edges is given by

$$\frac{1}{k} = \frac{1}{1b\pi EI} \left[a^2 - b^2 - \frac{4a^2b^2}{a^2b^2} \left(\ln \frac{a}{b}\right)^2 \right] \tag{57}$$

where a and b are the outer and inner radii, respectively. For a constant thickness, t,

$$I = \frac{t^3}{12(1 - \nu^2)} \tag{58}$$

For a sandwich fin as shown in Fig. 17 where only the structural value of the cladding is considered,

$$I = \frac{2(y_2^3 - y_1^3)}{3(1 - \nu^2)} \tag{59}$$

and the spring constant, K, per unit length of tube is given by

$$\frac{1}{K} = \frac{3(1 - \nu^2)}{32\pi nE(y_2^3 - y_1^3)} \left[a^2 - b^2 - \frac{4a^2b^2}{a^2-b^2} \left(\ln \frac{a}{b}\right)^2 \right] \tag{60}$$

where n is the number of fins per unit length.

Numerical Solution

A value for the dimensionless parameter $\eta L = L\sqrt{\frac{K}{EA}}$ is estimated for the following dimensions:

From Fig. 17, $y_2 = 0.005$ in.
$y_1 = 0.0025$ in.
$n = 15$ fins/in.

From Fig. 15, $A_o = \pi(r_o^2 - r_i^2) = 0.01276$ in^2
$A = \pi(r_f^2 - r_i^2) = 0.01897$ in^2
$b = r_f = 0.10375$ in.
$r_i = 0.06875$ in.

Figure 28 is a plot of ηL vs the diaphram outer radius a. The value of a lies between the center-to-center tube spacing and the tangent circle (Fig. 29). Selecting the value midway between these two,

$$a \approx \frac{2}{3} - \frac{b}{2} = 0.615 \text{ in.}$$

From Fig. 28 $\eta L \approx 1.8$.

The maximum stress in the finned tube, if the fins were to extend to the header, is plotted in Figs. 26 and 27 for the constant ΔT and linear ΔT respectively. For $\eta L = 1.8$ the maximum stresses are $0.68\,\alpha E \Delta T$ and $0.205\,\alpha E \Delta T_L$. For an unfinned tube length of 1.25 in., the maximum stresses in the unfinned tube are, from Eqs (49) and (54), $1.01\,\alpha E \Delta T$ and $0.300\,\alpha E \Delta T_L$, respectively. If ℓ is small compared to L, the stress in the unfinned tube is approximately the stress in the finned tube at x = 0, increased by the ratio of tube cross-sectional areas.

In the analysis above it was assumed that the section of tube between the fin matrix and header was straight and joined the header at right angles so that only tensile stresses were induced in the tube. In the actual design the tubes penetrate the circular header radially and are bent so as to enter the fixed matrix in parallel rows (Fig. 30).

An axial force, P, on the tube produces a bending moment Ps where the maximum moment-arm s is $1 - 1.750 \sin 30^\circ = 0.125$ in. The maximum axial stress in P/A_o and the maximum combined bending and axial stress is $Psr_o/I + P/A_o \cos 30^\circ$. The ratio of the combined stress to the maximum axial stress is $sr_oA_o/I + \cos 30^\circ$ and is equal to 4.33. Applying this correction to the previously calculated stresses in the unfinned tube, the maximum stresses are $4.38\,\alpha E \Delta T$ and $1.30\,\alpha E \Delta T_L$ for the constant ΔT and linear ΔT, respectively.

Because of the relatively high stresses produced from temperature differentials of the type considered above, the elastic stress-strain relations no longer apply. It becomes necessary to consider the actual shape of the stress-strain curve in order to estimate deformations and attempt to

predict the structural life under thermal strain cycling conditions. The criterion presently being used to predict structural life under strain cycling conditions is based on the work of L. F. Coffin[3] who was able to correlate failure of a tensile-compressive test specimen with the total accumulation of plastic strain. The total strain is made up of an elastic component and a plastic component, the magnitudes of which depend on the magnitude of the total strain, the stress-strain characteristics and stress relaxation properties of the material and the manner in which the strain is applied. For very large strains per cycle (greater than 0.1 percent) the elastic component is a negligible fraction of the total deformation. This permits the use of simplifying approximations to the actual stress strain curve in estimating the plastic strain per cycle and structural life. Figure 31 is a plot of the plastic strain per cycle against the number of cycles to failure for fine and coarse grained Inconel tubing at 1500°F. It is seen that strains of the order of 1 to 10 percent per cycle would be required to produce failure in a relatively small number of cycles.

The previously considered elastic problem is now analyzed from a consideration of the amount of plastic strain that would be induced in a tube which undergoes a temperature change with respect to surrounding tubes in the matrix. It was found that such a temperature differential produces a maximum tensile force in the unfinned tube in the region of the header and that large bending stresses could result if the tube has a slight degree of curvature where it joins the header as shown in Fig. 30. The elastic bending stress at the header connection was found to be a factor of four greater than the axial stress in the straight section of tube for the geometry shown. If the maximum stress at the header exceeds the elastic limit then yielding will be confined to a very small region adjacent to the header and relatively large strains can occur for a given deflection of the tube. Expressions were previously obtained for the relations between the force

3. L. F. Coffin, "A Study of the Effects of Cyclic Thermal Stresses on a Ductile Metal", Trans. ASME, 1954, p. 931.

and deflection of a tube at the edge of the fin matrix for a given temperature differential and are given by Eqs (55) and (56). A similar expression or "spring constant" will now be derived for the curved section of tube shown in Fig. 30 assumed in the elastic- plastic state. The two expressions can then be coupled to obtain the temperature differentials required to produce a given plastic-strain or structural lifetime.

A typical stress-strain diagram for a ductile material at high temperature is shown in Fig. 32 (solid line).

For strains of the magnitude considered above, the elastic portion of the curve can be neglected, and the curve can be approximated by the tangent line shown dotted in Fig. 32. The stress-strain law is then given by

$$\sigma = \sigma_o + E_t \epsilon \tag{61}$$

which assumes that no yielding takes place until the stress reaches the intercept value σ_o. Thereafter, stress is linearly proportional to strain and the constant of proportionality, E_t, is the slope of the tangent line, referred to as the tangent modulus. Deflection of the elastic portion of the tube will later be taken into account in determining the total deflection of the tube so that the idealized stress-strain law (Fig. 32) applies only to the plastic region.

Consider the section of tube shown in Fig. 33 subjected to a distributed bending moment, $M(\theta)$, produced by the force P. The applied moment at any point must be resisted by tensile and compressive forces acting over the cross sectional area of the tube so that

$$M(\theta) = \int_{area} \sigma(A) y dA \tag{62}$$

where y is the distance measured from the neutral axis to any incremental area acted upon by the force $\sigma(A)dA$. According to the idealized stress

strain law, no deformation of the tube will result until the bending moment reaches some critical value. In the region where the moment exceeds this value plastic deformation will result and the deflection equation is obtained from Eq (62) by substituting for stress the equivalent strain relation, Eq (61).

$$M(\theta) = \int_{area} \left[\sigma_o + E_t \epsilon(y) \right] y dA \tag{63}$$

Assuming that plane sections remain plane during bending,

$$\epsilon(y) = \frac{y}{\rho} = y \frac{d\phi}{ds} \quad , \tag{64}$$

where $1/\rho$ or $d\phi/ds$ is the curvature or change of slope with distance s along the curve and Eq (63) becomes

$$M(\theta) = \sigma_o \int_{area} y dA + E_t \frac{d\phi}{ds} \int_{area} y^2 dA \tag{65}$$

The first integral on the right is the first area moment and the second integral is the moment of inertia, I, of the cross section. If the product of the first moment and σ_o is set equal to M_o, then Eq (65) can be written

$$\frac{d\phi}{ds} = \frac{M(\theta) - M_o}{E_t I} \quad (\theta_e \leq \theta \leq x) \tag{66}$$

and the problem reduces to that of an "elastic" problem with the modulus of elasticity replaced with the tangent modulus. If the maximum moment is less than M_o no deformation will result.

Assume that the moment produced from the force P in Fig. 33 reaches the value of M_o at some point along the tube defined by the angle $\theta = \theta_e$.

In the region $\theta_e \leq \theta \leq \psi$ psi the bending moment exceeds M_o, and the tube deforms according to Eq (66). The bending moment is given by

$$M(\theta) = PR(1 - \cos\theta)$$

so that the angle at which plastic deformation begins is

$$\theta_e = \cos^{-1}\left(1 - \frac{M_o}{PR}\right) \tag{67}$$

The deflection of the tube in the direction of the force P is obtained from the strain-energy relation

$$u_p = \frac{\partial U}{\partial P} = \int_s \frac{M}{E_t I}\frac{\partial M}{\partial P}\, ds \tag{68}$$

where the integral is taken over the length of tube defined by the angle θ_p, and the moment is

$$M(\theta) - M_o = PR(\cos\theta_e - \cos\theta) \tag{69}$$

Deflection of the elastic portion of the tube can be included to give the total deflection $u_o = u_e + u_p$.

Substituting Eq (69) into Eq (68), the plastic component of deflection is given by

$$u_p = \frac{PR^3}{E_t I}\int_{\theta_e}^{\psi} (\cos\theta_e - \cos\theta)^2\, d\theta$$

$$= \frac{PR^3}{E_t I}\left[(\psi-\theta_e)\cos^2\theta_e - (\sin\psi - \sin\theta_e)2\cos\theta_e + \frac{\psi - \theta_e}{2} + \frac{1}{4}(\sin 2\psi - \sin 2\theta_e)\right] \tag{70}$$

The elastic component of deflection is obtained from a similar integration and is equal to

$$u_e = \frac{PR^3}{EI}\left[\frac{3}{2}\theta_e - 2\sin\theta_e + \frac{\sin 2\theta_e}{4}\right] \tag{71}$$

The maximum plastic strain occurs at the fixed end and is given by

$$\epsilon_{max} = \frac{\left[M(x) - M_o\right] r_o}{E_t I}$$

From Eqs (67) and (69),

$$\epsilon_{max} = \frac{PRr_o(\cos\theta_e - \cos\psi)}{E_t I} = \frac{r_o}{E_t I}\left[PR(1 - \cos\psi) - M_o\right] \qquad (72)$$

From the curve of Fig. 31 a value of plastic strain per cycle can be selected for a specified lifetime. The force, P, required to produce this strain can be obtained from Eq (72) and the corresponding deflection from Eqs (70) and (71). The temperature differentials necessary to produce the calculated force and deflection can then be obtained from the matrix "spring constants", Eqs (55) and (56).

Numerical Solution

From Fig. 30: $\psi = 30^o$, $R = 0.933$ in.

$$R(1 - \cos 30^o) = 1 - 1.1750 \sin 30^o$$

For the unfinned tube: $r_o = 0.09375$ in., $r_i = 0.06875$ in.

$I_o = 0.4312\text{x}10^{-4}$ in^4 , $\int_A y dA = 6.654\text{x}10^{-4}$ in^3 .

The tangent modulus approximation to the stress-strain curve for Inconel at 1500°F gives for the intercept and slope (Fig. 32),

$\sigma_o = 18{,}800$ psi $\qquad E_t = 2.73\text{x}10^{-4}$ psi

The minimum bending moment required for yielding to take place is

$$M_o = \sigma_o \int_A dyA = 12.51 \text{ lb in.}$$

If we select a value of 10 percent for ϵ_p which, from Fig. 31, corresponds to approximately 40 cycles to failure, then the required axial force P of 105 lb is obtained from Eq (72). In this equation ϵ_{max} is one-half the strain per cycle of 5 percent. From Eq (67), the angle θ_e which locates the point of transition from elastic to plastic deformation (Fig. 32) is 0.5106 radians or 29.26°. This corresponds to a plastic region of only 0.73° or, in terms of tube length, 0.0121 in. Since the angle θ_e differs from ψ by such a small amount, the plastic component of deformation (Eq 70) can be more readily calculated by approximating the trigonometric functions of this incremental angle by the first two terms of their series expansions. If θ represents this difference then Eq (70) reduces to

$$u_p = \frac{PR^3}{E_t I}\left[\frac{(\Delta\theta)^3}{3}\sin^2\theta_e - \frac{(\Delta\theta)^4}{4}\sin\theta_e\cos\theta_e\right]$$

Substituting the above values for P and $\Delta\theta$ into this expression gives for u_p, $1.25\text{x}10^{-5}$ in. The elastic component of displacement is calculated from Eq (71) to be $1.85\text{x}10^{-4}$ in. The temperature differentials required to produce these displacements are obtained from Eq (55) and Eq (56). In terms of total displacement, u_o, and axial force, P, the temperature differentials are given by

$$\Delta T = 0.387\ P + 1.68\text{x}10^4 u_o$$

$$\Delta T_L = 1.29\ P + 5.59\text{x}10^4 u_o$$

for the step ΔT and linear ΔT respectively. For u_o and P equal to $1.98\text{x}10^{-4}$ in. and 105 lb, respectively, the above temperature differentials are 44°F and 147°F, respectively, corresponding to about 40 thermal cycles to produce failure. If the calculations are repeated for 1 percent plastic strain per cycle corresponding to a structural life of approximately 300 cycles, the required temperature differentials are 42°F and 141°F for the step ΔT and linear ΔT, respectively. The sensitivity of the number of cycles to produce failure with temperature difference is a consequence of

the lack of strain hardening at these high temperatures. Once plastic yielding begins very large strains can be realized from a slight increase in the stress level as evidenced from the relatively small slope of the stress-strain curve in the plastic region. The slope is also quite dependent on strain rate at these temperatures. This effect was not included in the above analysis so that these results would only strictly apply to a condition where the rate of application of the temperature differential is equal to the strain rate of the tensile specimen from which the stress-strain curve was obtained.

Another thermal stress problem considered was the effect of a temperature differential between the header drum and adjacent fins. The unfinned portion of tubes shown in Fig. 34 will be subjected to bending as a result of this temperature differential. Assuming that the fins are rigid, an individual tube will deform as shown in Fig. 35. From symmetry, the length $\ell/2$ behaves as a fixed-ended cantilever beam subjected to an end load which results in a maximum displacement of $\alpha\Delta TL/4$. We are interested in determining the allowable dimensions, ℓ and L which will enable the unit to withstand strain-cycling conditions for a predicted temperature differential, ΔT.

The problem is analogous to the one previously considered where a cantilever beam is stressed beyond the elastic range so that a portion of the beam undergoes plastic deformation. If ℓ_e and ℓ_p are the length of the elastic region and plastic region respectively, then the deflection at the free end is given by

$$y(o) = \frac{P\ell_e^3}{3EI} + \frac{P}{E_tI}\left(\frac{\ell_p^3}{3} + \frac{\ell_e\ell_p^2}{2}\right) \tag{73}$$

where plastic yielding is described by the tangent modulus approximation (Fig. 32). The maximum strain at the fixed end is

$$\epsilon_{max} = \frac{P\ell_p r_o}{E_tI} \tag{74}$$

and the relative tube lengths are defined by

$$\ell_e = \frac{\ell}{2} - \ell_p = \frac{M_o}{P}, \tag{75}$$

where M_o was shown to be equal to the product of the intercept, σ_o, of the stress-strain tangent curve and the first moment of the tube cross sectional area about the neutral axis. If y(o) is set equal to the maximum displacement, $\alpha\Delta TL/4$, and combined with Eqs (74) and (75), the following expression is obtained which relates the dimensions ℓ and L to the maximum strain and temperature differential:

$$\Delta T = \frac{\epsilon_{max}\ell^2}{3\alpha L r_o}\left[1 - \frac{1}{2\beta} - \frac{1}{2\beta^2}\right] + \frac{\epsilon_{max}E_t\ell^2}{3\alpha L r_o E\beta^2}\left[\frac{1}{\beta - 1}\right] \tag{76}$$

where

$$B \equiv 1 + \frac{\epsilon_{max}E_t I}{M_o r_o}$$

This result is plotted in Fig. 36 for 1 percent strain per cycle ($\epsilon_{max} = 0.005$) corresponding to approximately 300 cycles to failure from Fig. 30. The modulus of elasticity and tangent modulus were taken as 18×10^6 psi and 2.73×10^4 psi, respectively; the coefficient of thermal expansion was taken as 10^{-5} in/in^{o}F and the moment of inertia and tube outer radius correspond to 3/16 in. O.D. x 25 mil wall tubing.

UNCLASSIFIED
ORNL-LR-DWG. 27323

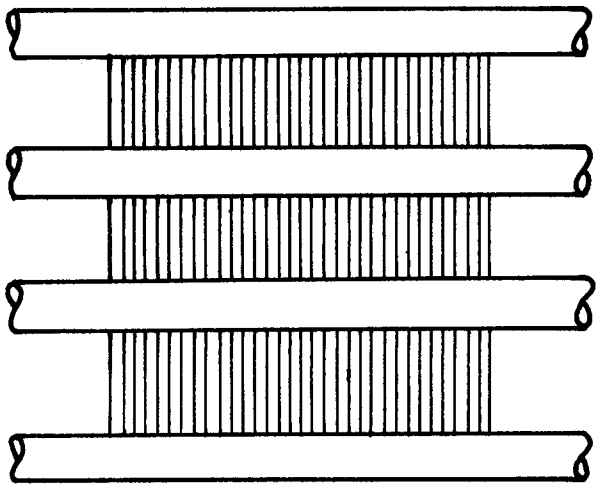

FIGURE 1

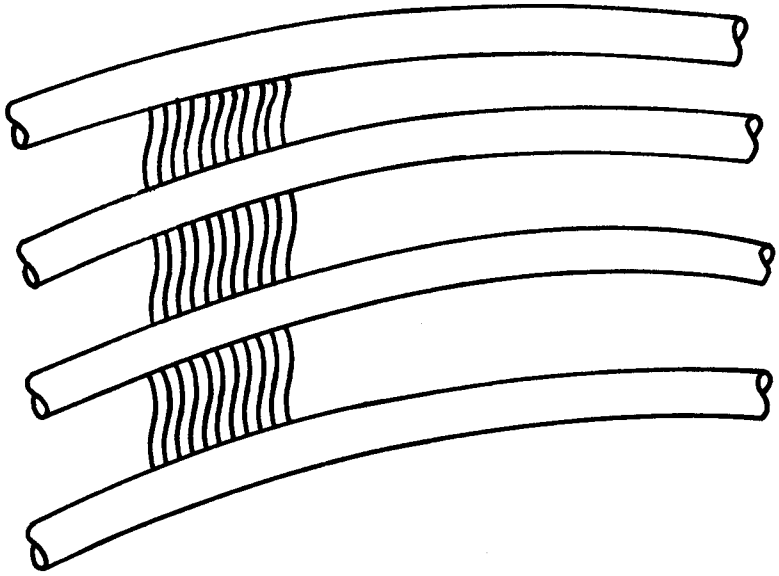

FIGURE 2

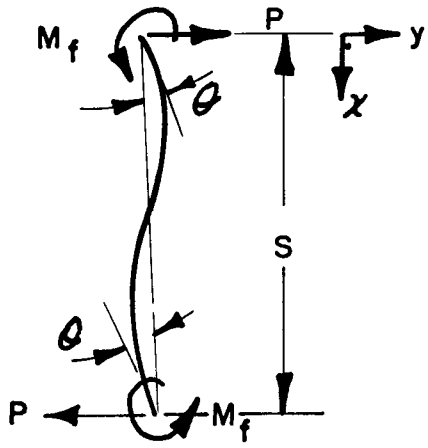

FIGURE 3

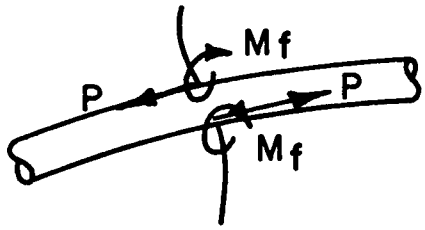

FIGURE 4

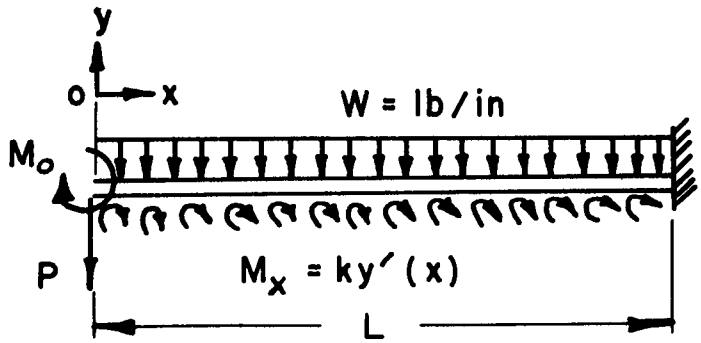

FIGURE 5

UNCLASSIFIED
ORNL-LR-DWG. 27326

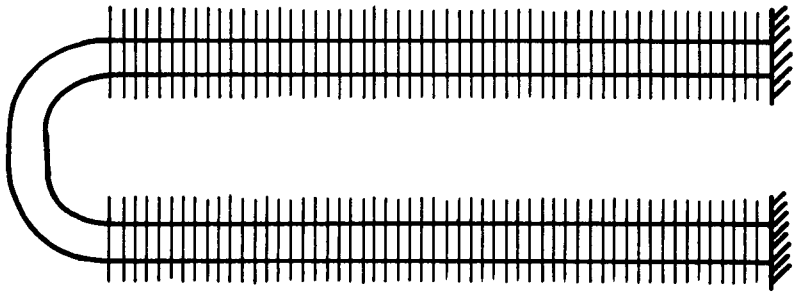

FIGURE 6

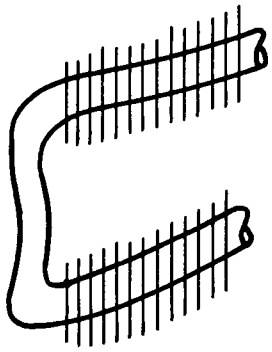

FIGURE 7

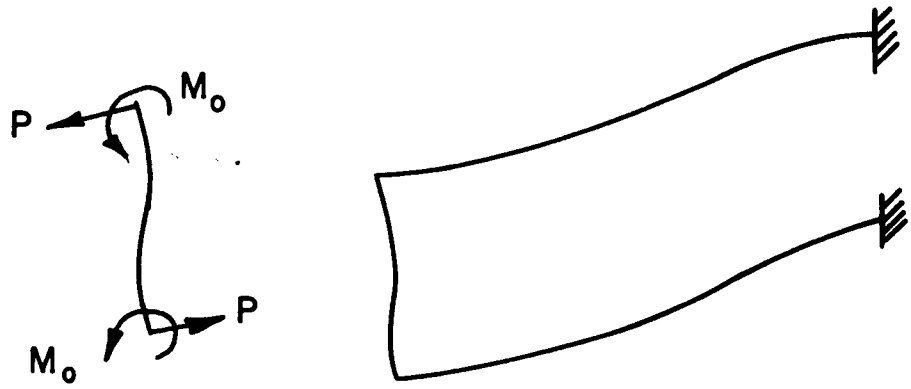

FIGURE 8

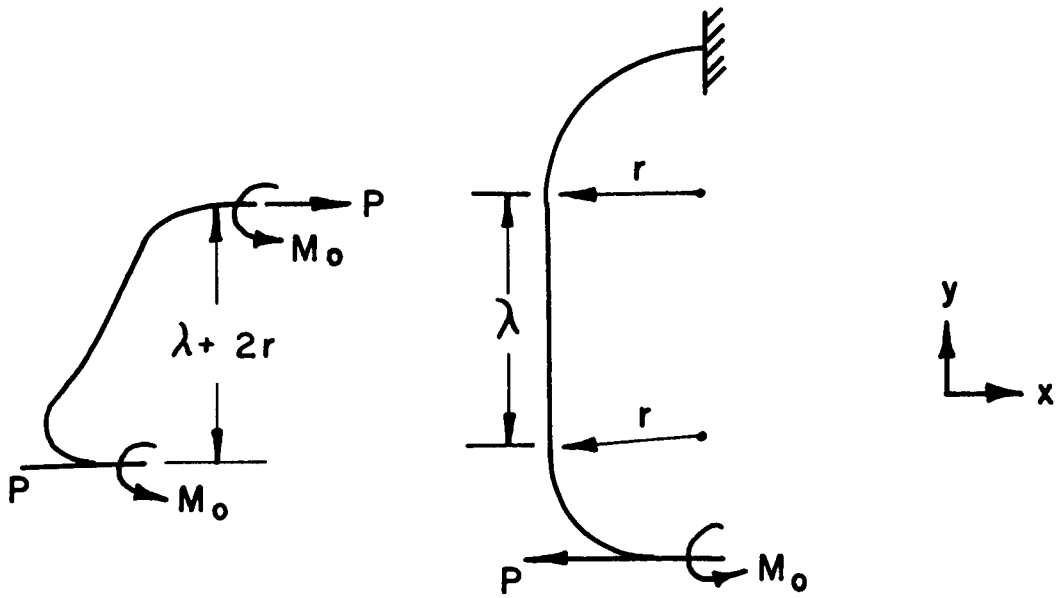

FIGURE 9

UNCLASSIFIED
ORNL-LR-DWG. 27328

FIGURE 10

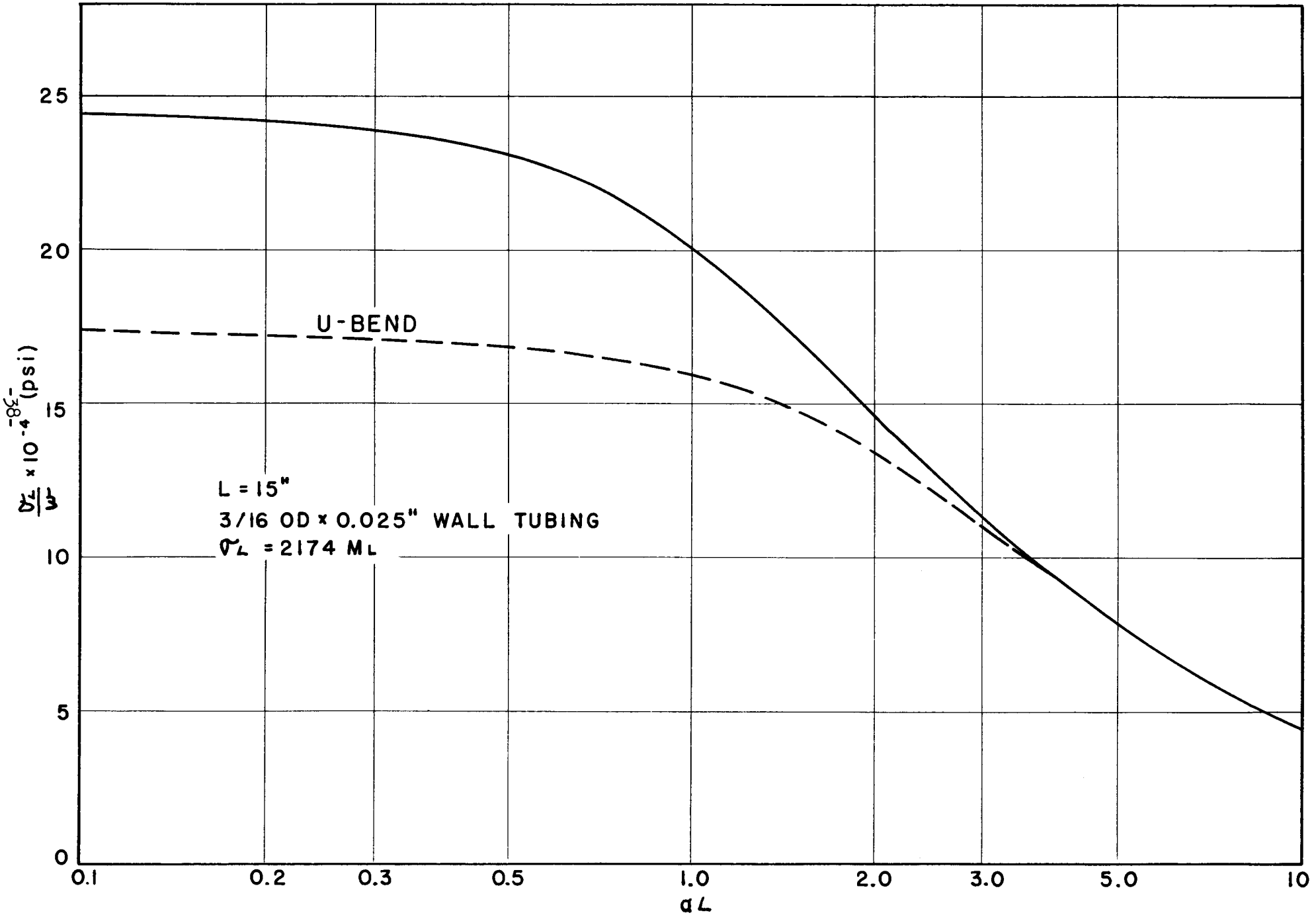

UNCLASSIFIED
ORNL-LR-DWG. 27329

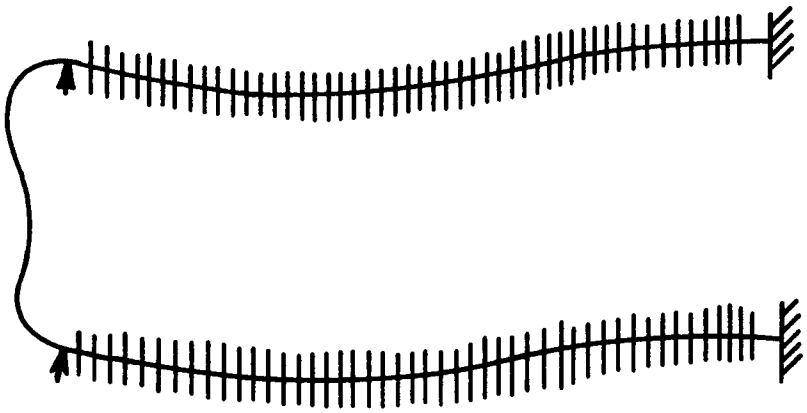

FIGURE 11

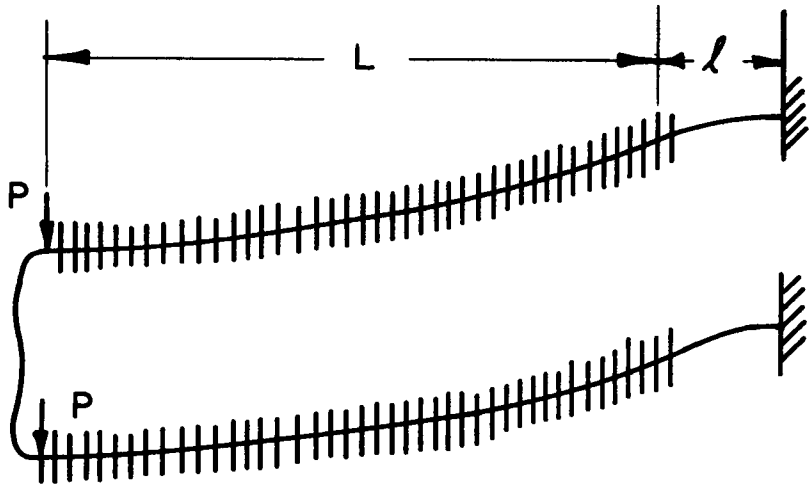

FIGURE 12

UNCLASSIFIED
ORNL-LR-DWG. 27331

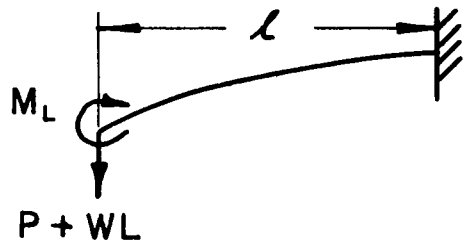

FIGURE 13

UNCLASSIFIED
ORNL-LR-DWG. 27332

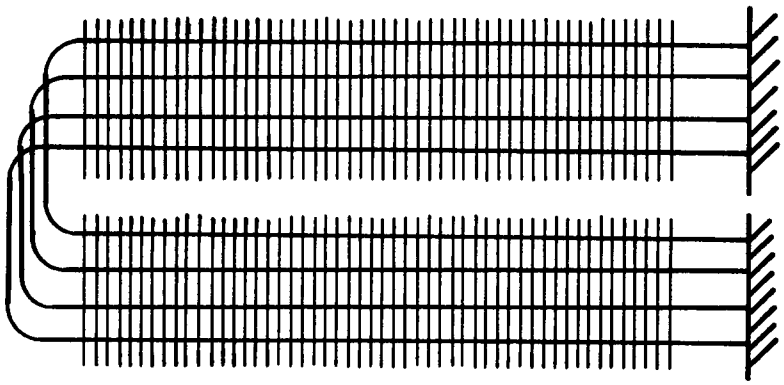

FIGURE 14

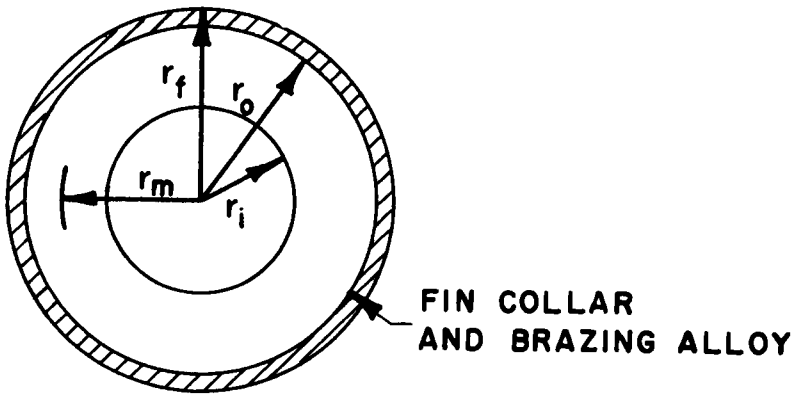

FIGURE 15

UNCLASSIFIED
ORNL-LR-DWG. 27333

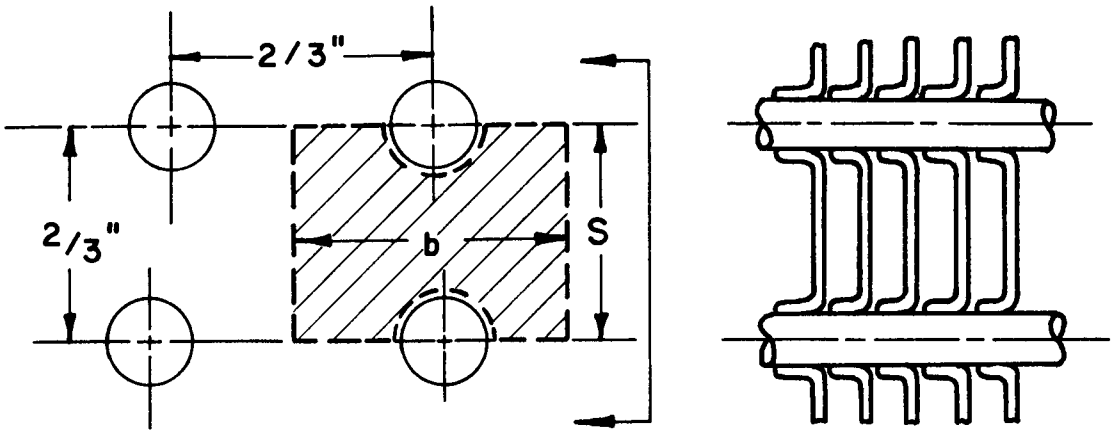

FIGURE 16

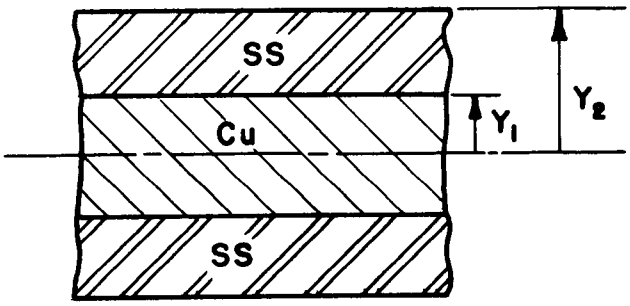

FIGURE 17

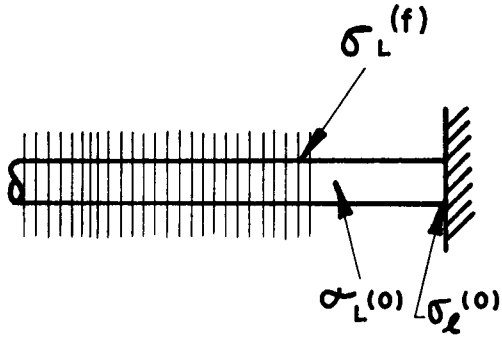

FIGURE 18

UNCLASSIFIED
ORNL-LR-DWG. 27335

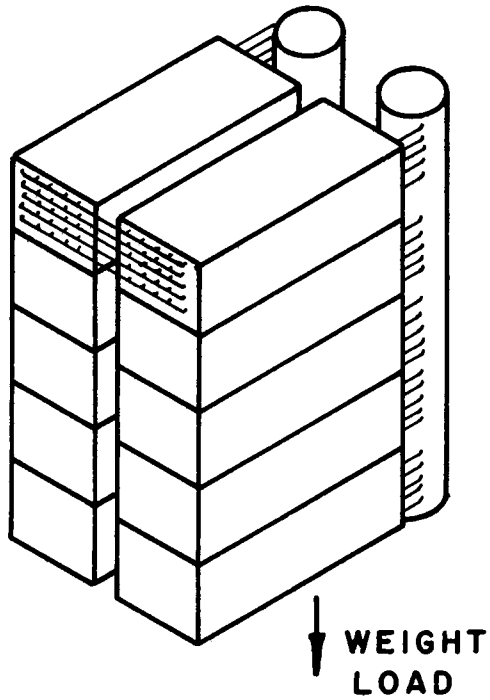

FIGURE 19

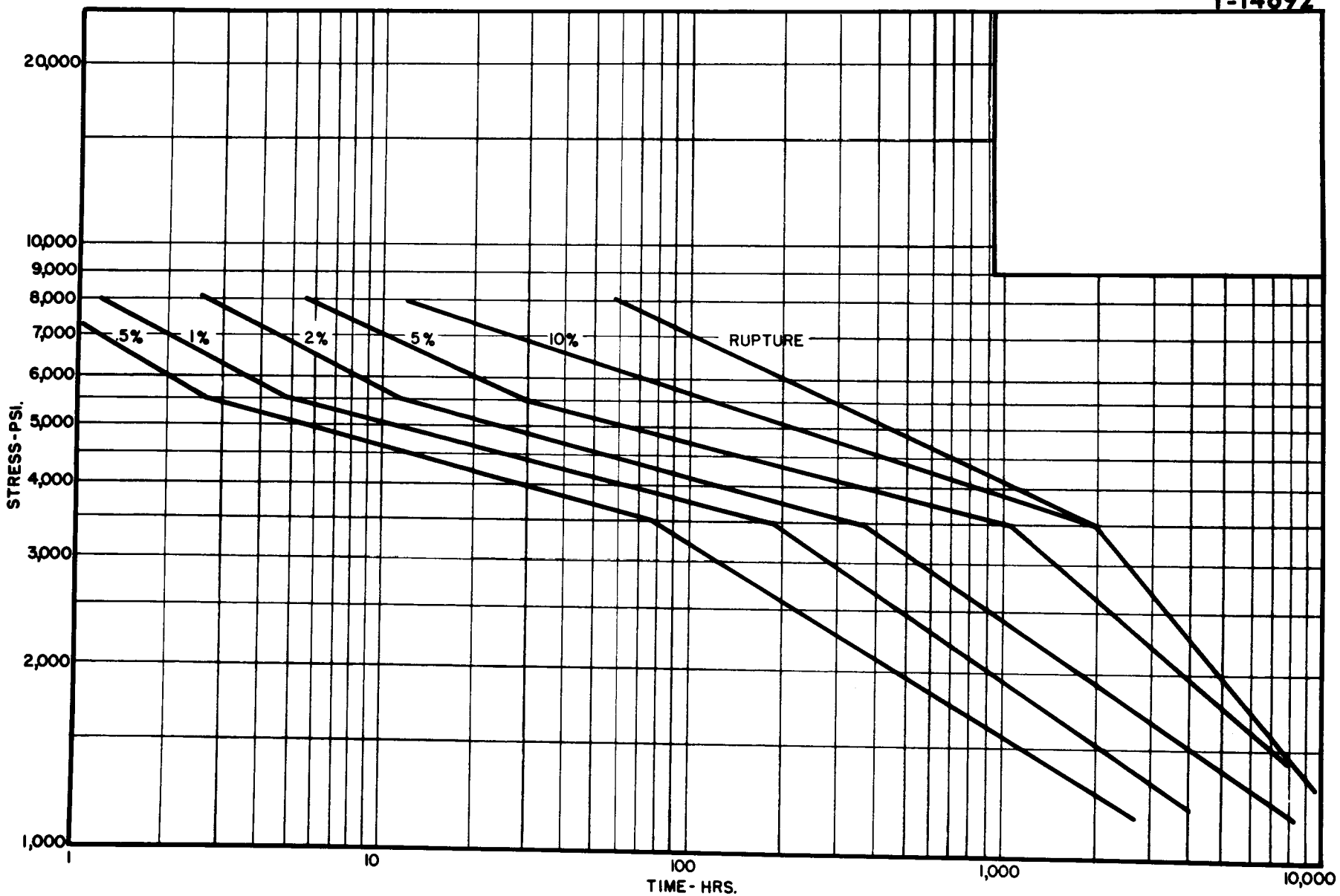
20,000
10,000
9,000
8,000
7,000
6,000
5,000
4,000
3,000
2,000
1,000
STRESS-PSI.
.5%
1%
2%
5%
10%
RUPTURE
1
10
100
1,000
10,000
TIME-HRS.

FIGURE 20

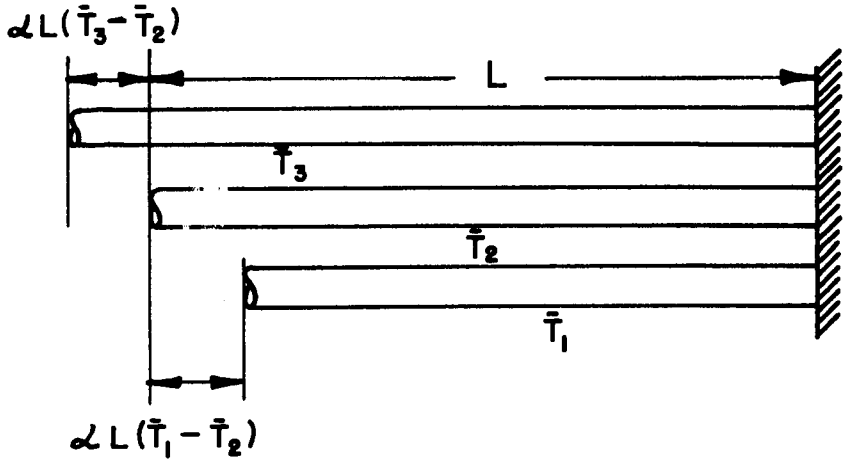

FIGURE 21

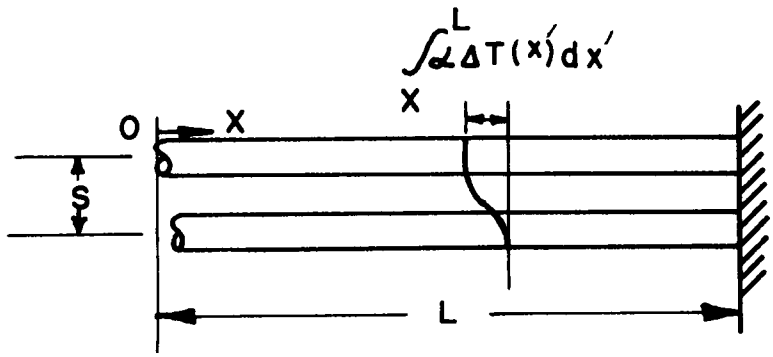

FIGURE 22

[redacted]

ORNL-LR-DWG. 27337

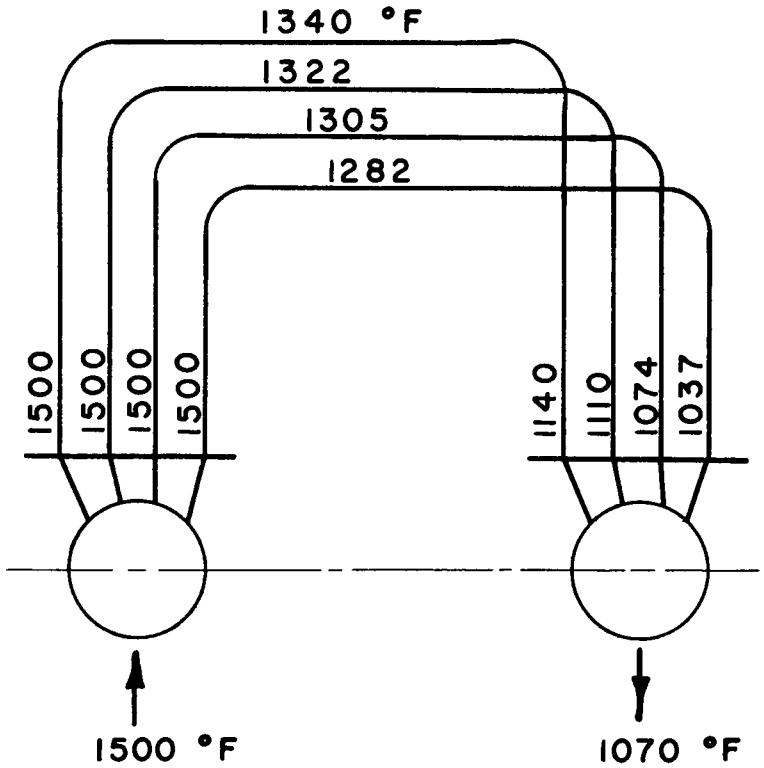

FIGURE 23

UNCLASSIFIED
ORNL-LR-DWG. 27338

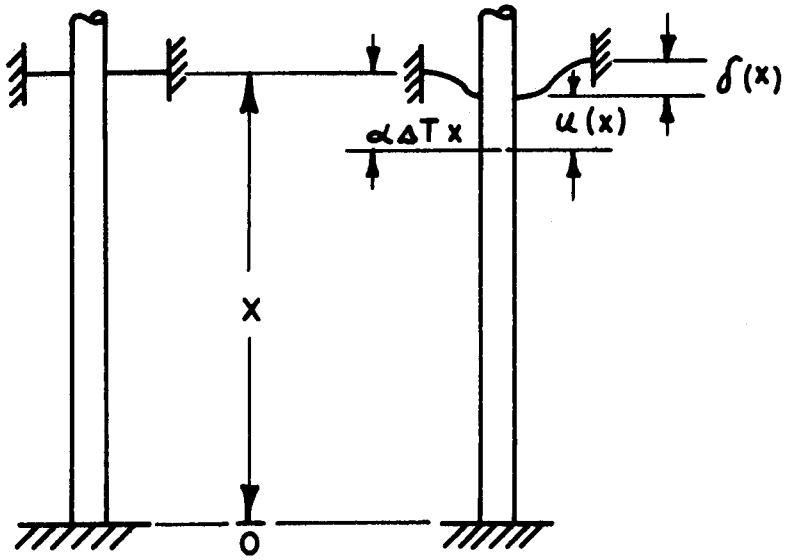

FIGURE 24

UNCLASSIFIED
ORNL-LR-DWG. 27339

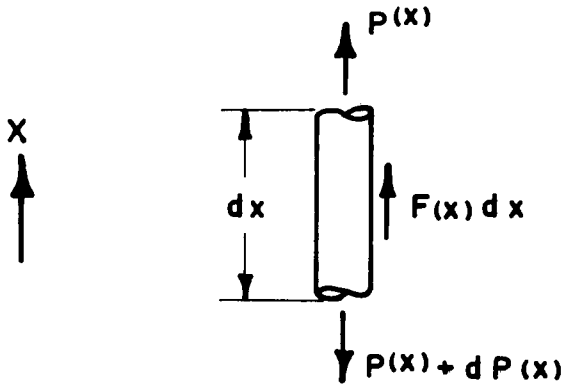

FIGURE 25

UNCLASSIFIED
ORNL-LR-DWG. 27340

FIGURE 26

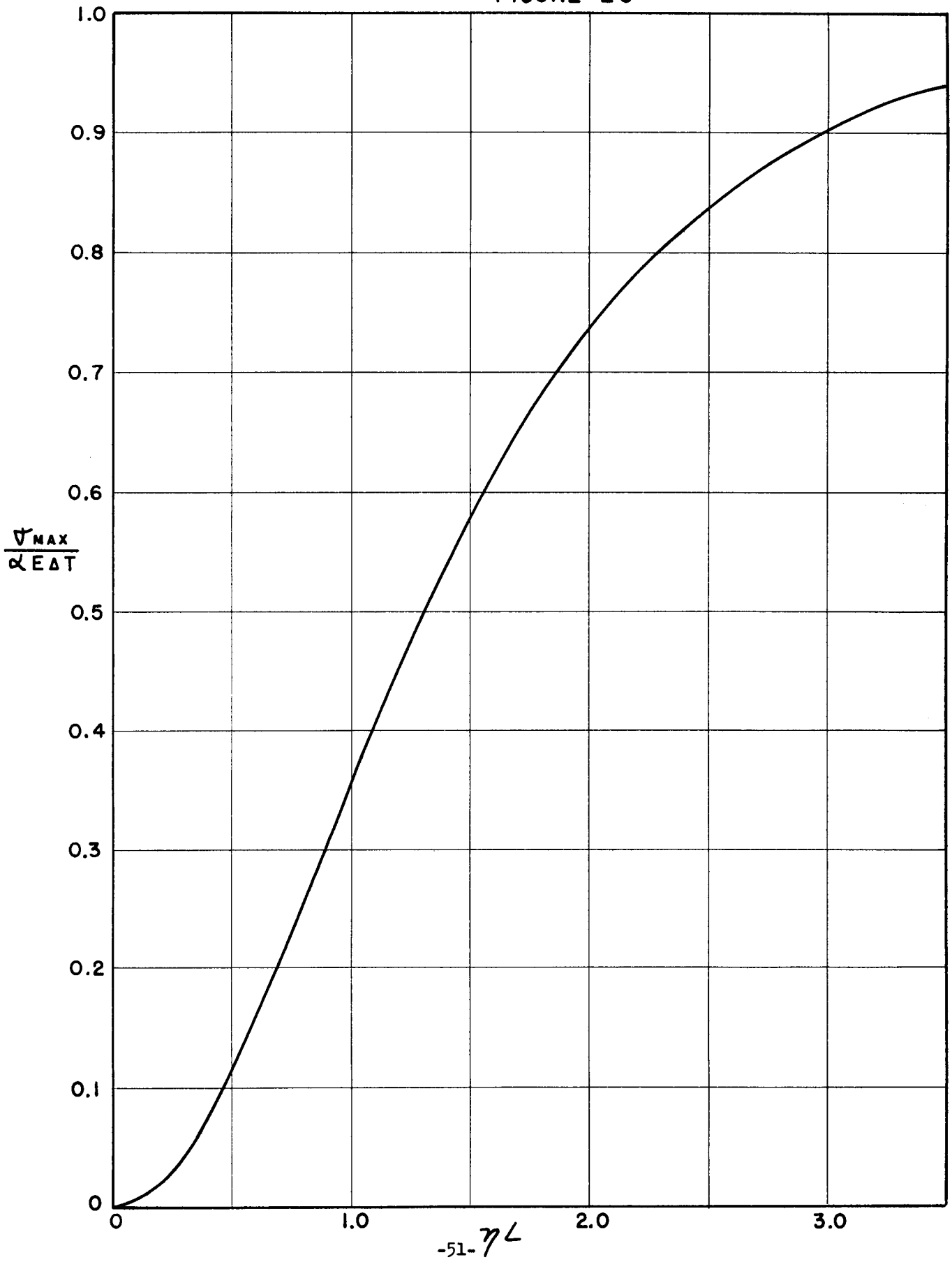

FIGURE 27

UNCLASSIFIED
ORNL-LR-DWG. 27341

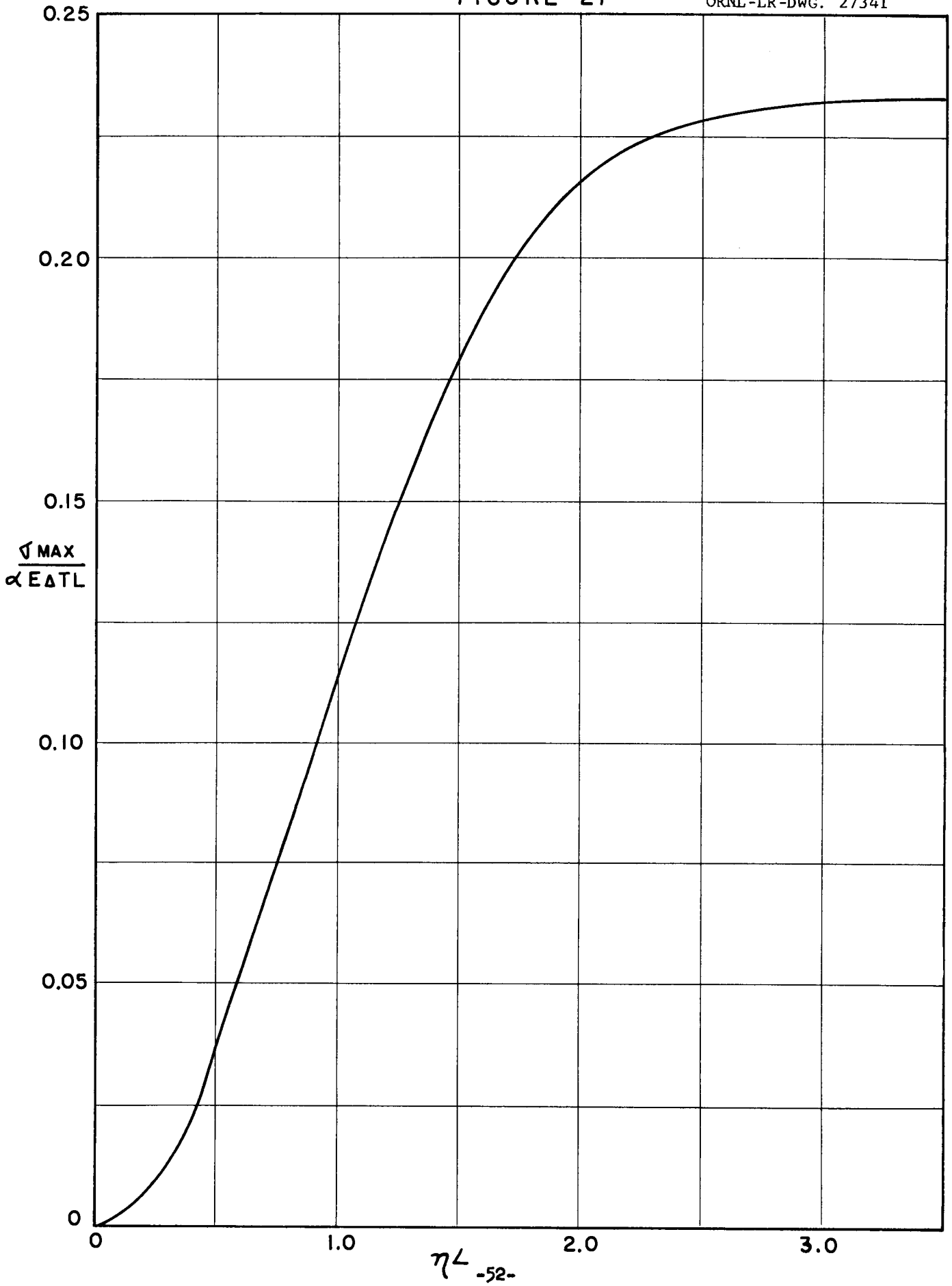

FIGURE 28

UNCLASSIFIED
ORNL-LR-DWG. 27342

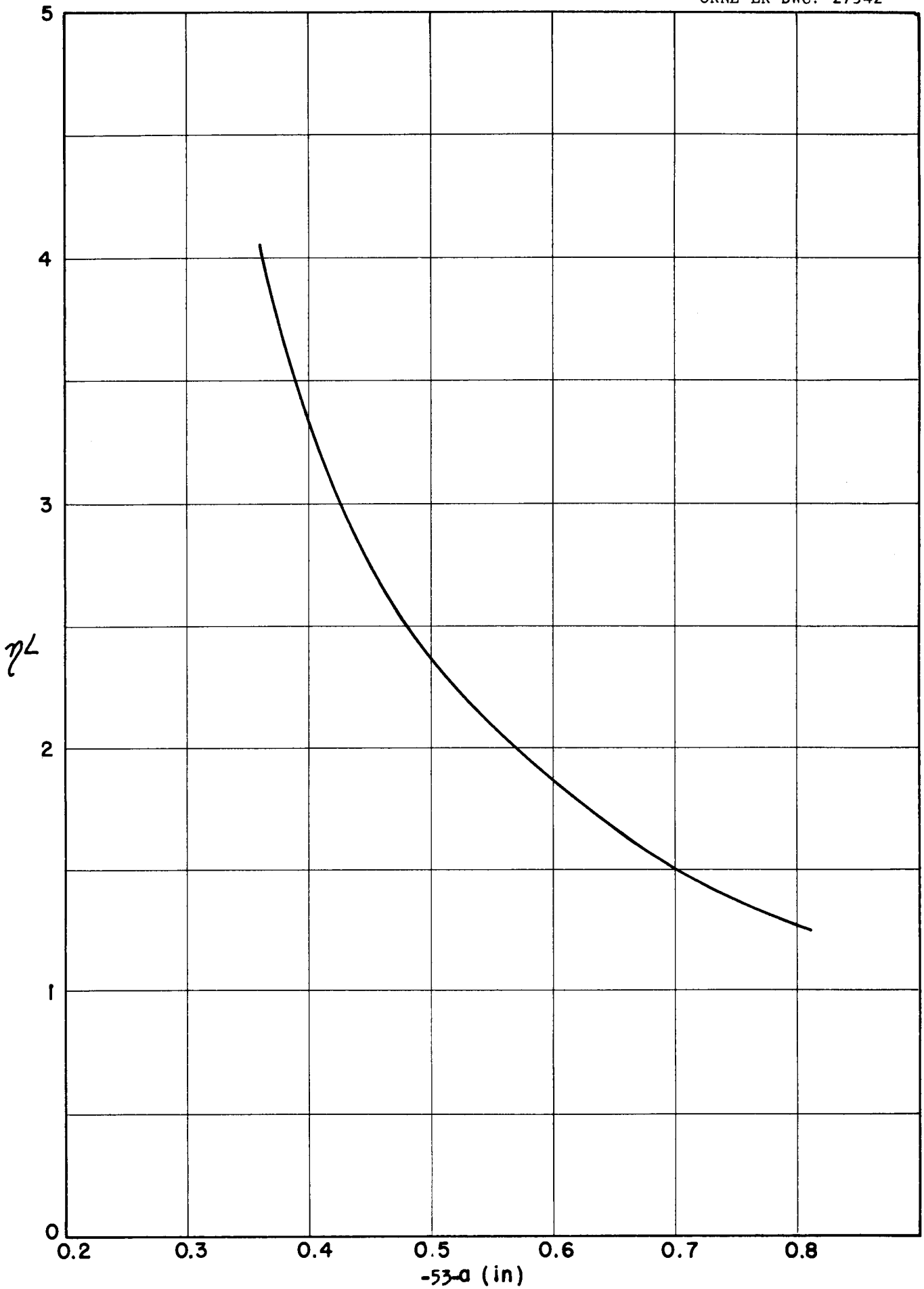

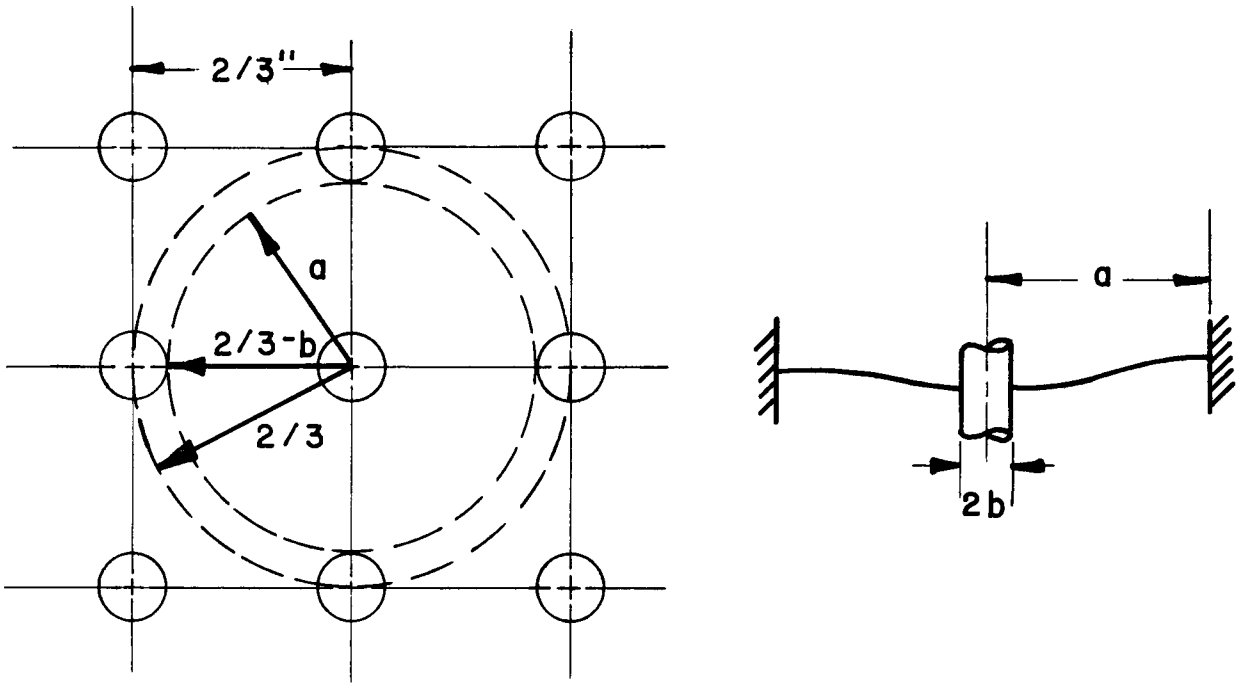

FIGURE 29

UNCLASSIFIED
ORNL-LR-DWG. 27344

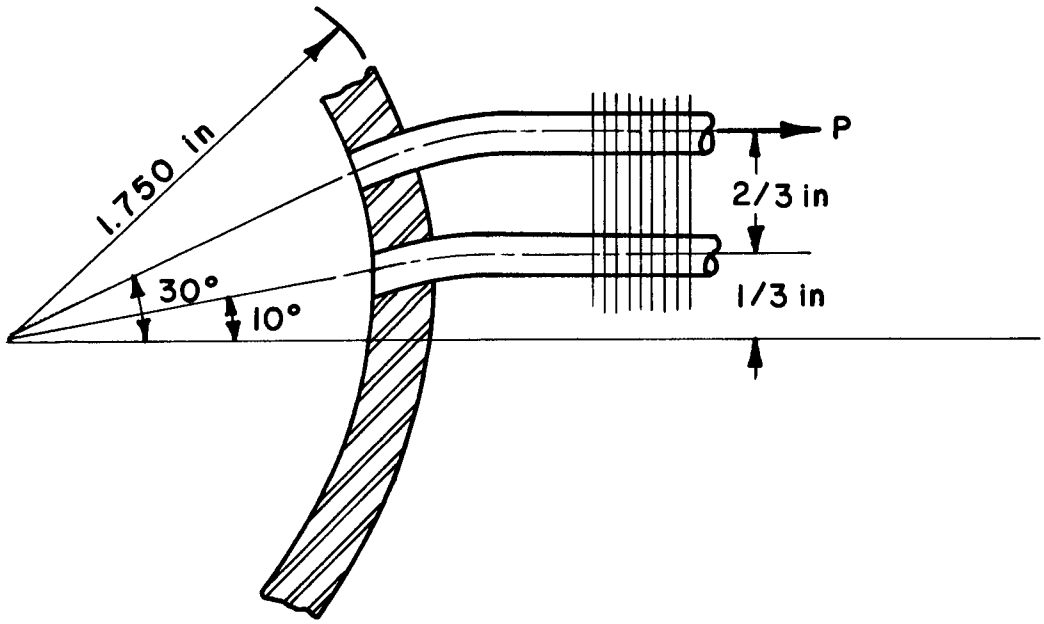

FIGURE 30

UNCLASSIFIED
PHOTO 28203

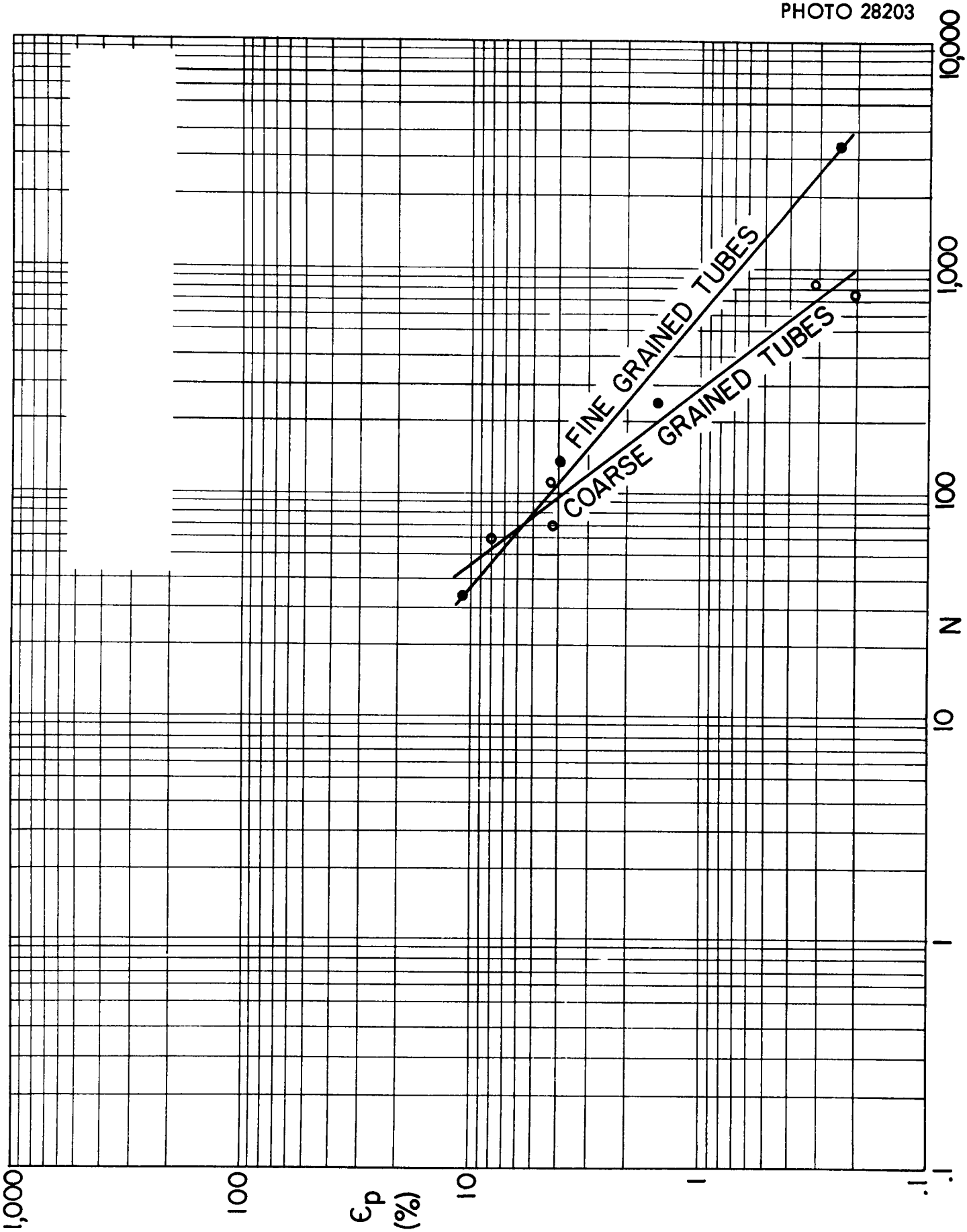

FIGURE 31

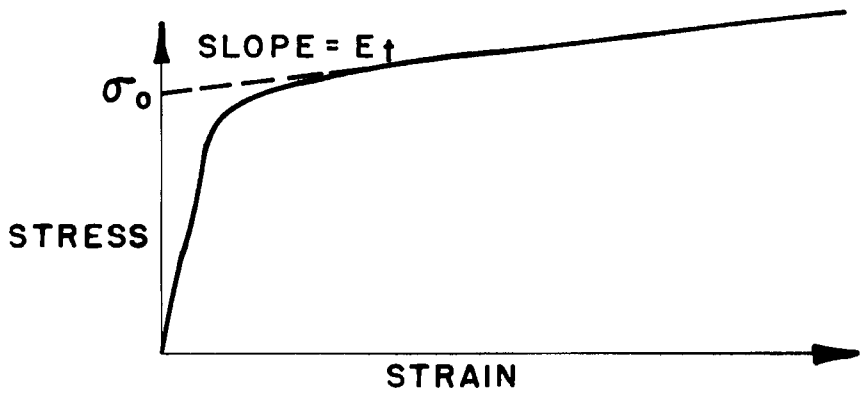

FIGURE 32

UNCLASSIFIED
ORNL-LR-DWG. 27346

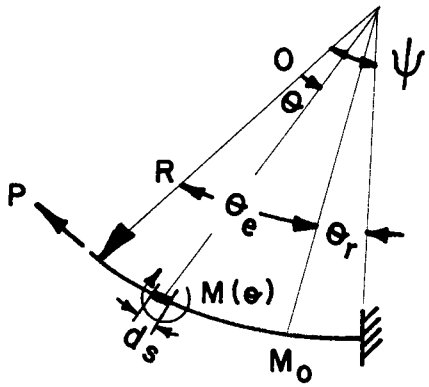

FIGURE 33

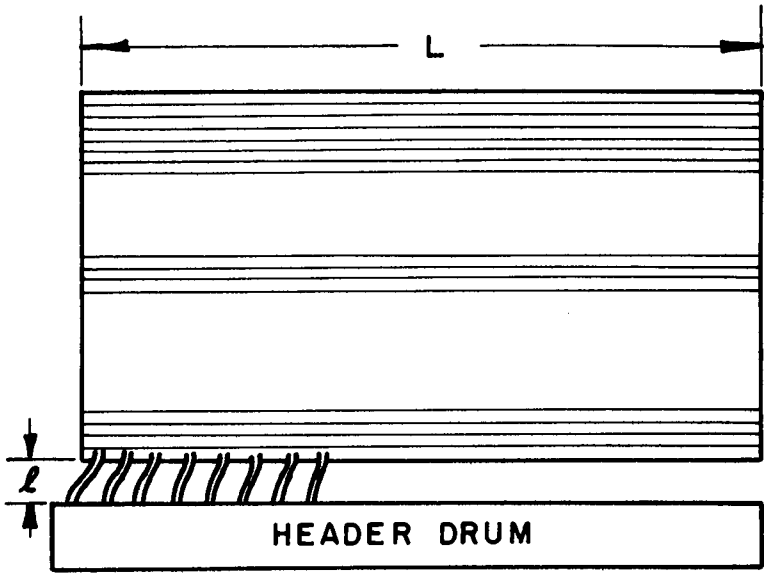

FIGURE 34

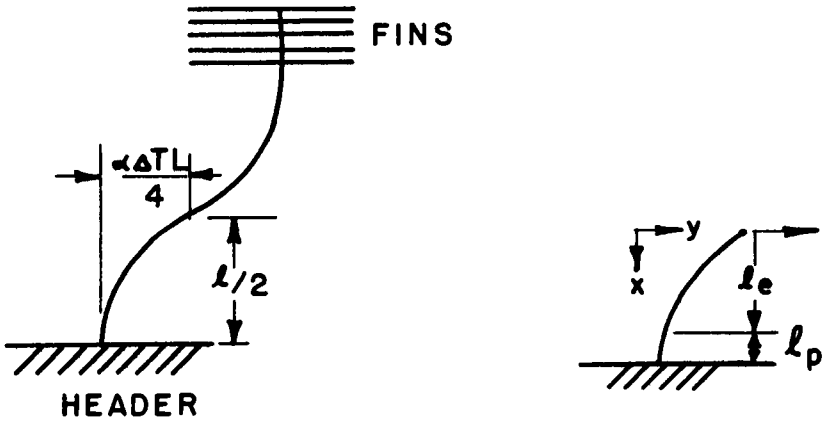

FIGURE 35

FIGURE 36

UNCLASSIFIED
ORNL-LR-DWG. 27348

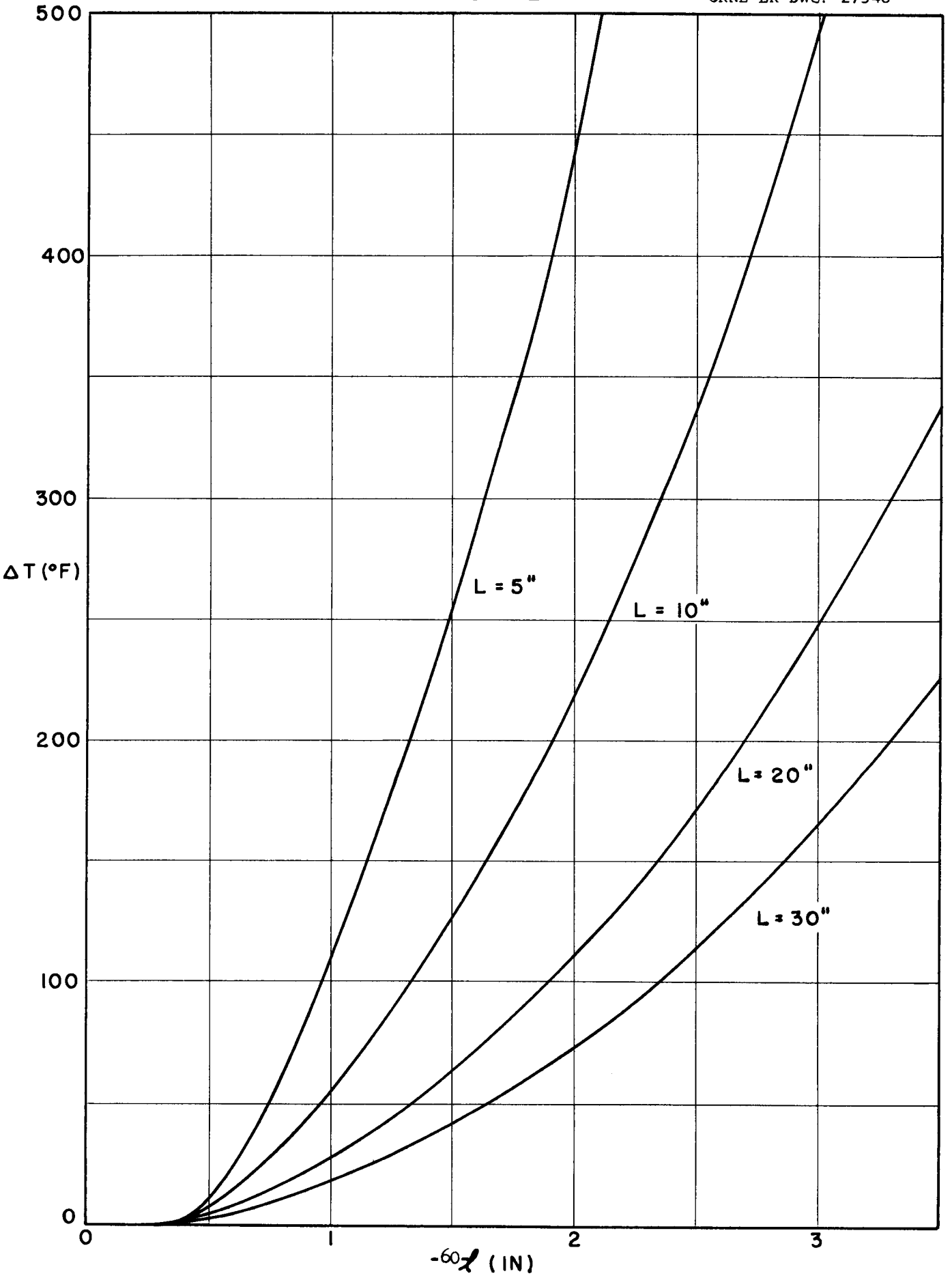

INTERNAL DISTRIBUTION

1. J. C. Amos
2. D. S. Billington
3. F. F. Blankenship
4. E. P. Blizard
5. A. L. Boch
6. C. J. Borkowski
7. G. E. Boyd
8. E. J. Breeding
9. R. B. Briggs
10. D. W. Cardwell
11. C. E. Center (K-25)
12. R. A. Charpie
13. B. Y. Cotton
14. F. L. Culler
15. J. H. DeVan
16. D. A. Douglas
17. L. B. Emlet (K-25)
18. D. E. Ferguson
19. A. P. Fraas
20. J. H. Frye, Jr.
21. W. T. Furgerson
22. R. J. Gray
23. B. L. Greenstreet
24. W. R. Grimes
25. E. Guth
26. C. S. Harrill
27. R. L. Heestand
28. H. W. Hoffman
29. A. Hollaender
30. A. S. Householder
31. W. H. Jordan
32. P. R. Kasten
33. G. W. Keilholtz
34. M. T. Kelley
35. J. L. Kerrebrock
36. J. A. Lane
37. R. S. Livingston
38. H. G. MacPherson
39. R. E. MacPherson
40. W. D. Manly
41. J. R. McNally
42. R. V. Meghreblian
43. K. Z. Morgan
44. E. J. Murphy
45. J. P. Murray (Y-12)
46. M. L. Nelson
47. P. Patriarca
48. A. M. Perry
49. H. W. Savage
50. A. W. Savolainen
51. R. D. Schultheiss
52. R. L. Senn
53. E. D. Shipley
54. M. J. Skinner
55. A. H. Snell
56. F. J. Stanek
57. J. A. Swartout
58. A. Taboada
59. J. R. Tallackson
60. E. H. Taylor
61. D. B. Trauger
62. A. M. Weinberg
63. C. E. Winters
64. M. M. Yarosh

65-67. ORNL - Y-12 Technical Library, Document Reference Section
68-75. Laboratory Records Department
76. Laboratory Records ORNL R.C.
77-79. Central Research Library
80. Reactor Experimental Engineering Library

EXTERNAL DISTRIBUTION

81. Division of Research and Development, AEC, ORO
82-84. Air Force Ballistic Missile Division
85-86. AFPR, Boeing, Seattle
87. AFPR, Boeing, Wichita
88. AFPR, Curtiss-Wright, Clifton
89. AFPR, Douglas, Long Beach
[illegible]-92. AFPR, Douglas, Santa Monica

93. AFPR, Lockheed, Burbank
94-95. AFPR, Lockheed, Marietta
96. AFPR, North American, Canoga Park
97. AFPR, North American, Downey
98-99. Air Force Special Weapons Center
100. Air Materiel Command
101. Air Research and Development Command (RDGN)
102. Air Research and Development Command (RDTAPS)
103-116. Air Research and Development Command (RDZPSP)
117. Air Technical Intelligence Center
118-120. ANP Project Office, Convair, Fort Worth
121. Albuquerque Operations Office
122. Argonne National Laboratory
123. Armed Forces Special Weapons Project, Sandia
124. Armed Forces Special Weapons Project, Washington
125. Assistant Secretary of the Air Force, R&D
126-131. Atomic Energy Commission, Washington
132. Atomics International
133. Battelle Memorial Institute
134-135. Bettis Plant (WAPD)
136. Bureau of Aeronautics
137. Bureau of Aeronautics General Representative
138. BAR, Aerojet-General, Azusa
139. BAR, Convair, San Diego
140. BAR, Glenn L. Martin, Baltimore
141. BAR, Grumman Aircraft, Bethpage
142. Bureau of Yards and Docks
143. Chicago Operations Office
144. Chicago Patent Group
145. Curtiss-Wright Corporation
146. Engineer Research and Development Laboratories
147-150. General Electric Company (ANPD)
151. General Nuclear Engineering Corporation
152. Hartford Area Office
153. Idaho Operations Office
154. Knolls Atomic Power Laboratory
155. Lockland Area Office
156. Los Alamos Scientific Laboratory
157. Marquardt Aircraft Company
158. Martin Company
159. National Advisory Committee for Aeronautics, Cleveland

160. National Advisory Committee for Aeronautics, Washington
161. Naval Air Development Center
162. Naval Air Material Center
163. Naval Air Turbine Test Station
164. Naval Research Laboratory
165. New York Operations Office
166. Nuclear Development Corporation of America
167. Nuclear Metals, Inc.
168. Office of Naval Research
169. Office of the Chief of Naval Operations (OP-361)
170. Patent Branch, Washington
171-174. Pratt and Whitney Aircraft Division
175. San Francisco Operations Office
176. Sandia Corporation
177. School of Aviation Medicine
178. Sylvania-Corning Nuclear Corporation
179. Technical Research Group
180. USAF Headquarters
181. USAF Project RAND
182. U.S. Naval Radiological Defense Laboratory
183-184. University of California Radiation Laboratory, Livermore
185-202. Wright Air Development Center (WCOSI-3)
203-227. Technical Information Service Extension, Oak Ridge